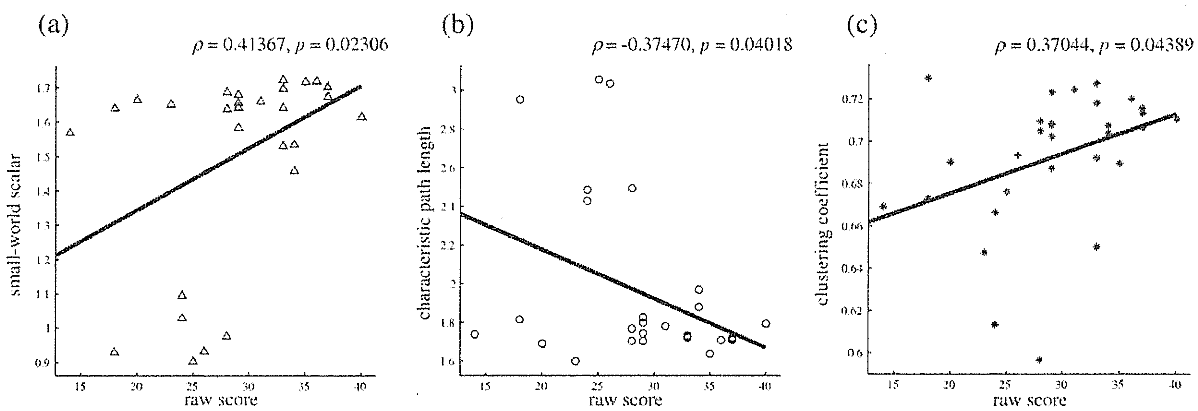

Fig. 8. Regression lines of the graph indices on sub-networks. The average degree of all sub-network graphs was 8. (a) The regression line between the small-world scalar and the raw score of the simultaneous processing scale (ρ = 0.41367, p = 0.02306), (b) that between L and the raw score (ρ = −0.37470, p = 0.04018), and (c) that between C and the raw score (ρ = 0.37044, p = 0.04389). The solid lines indicate that all graph indices are well associated with the raw score of the simultaneous processing scale.

psychiatric history in studies of encephalopathy, as "well-functioning." In previous studies of functional networks in the resting state, the networks of well-functioning brains showed stronger small-worldness than others did (Micheloyannis, Pachou, Stam, Breakspear et al., 2006; Stam et al., 2007; van den Heuvel et al., 2009). In the work of van den Heuvel et al. (2009), the result of functional magnetic resonance imaging (fMRI) demonstrated that in the resting state, the IQ of adults showed a negative correlation with the normalized path length. Stronger small-worldness was observed in participants with a high IQ than in participants with a low IQ. Children's and young adults' brain networks possess similar small-world organization (Supekar et al., 2009).

However, the results on the simultaneous processing raw score of children showed the opposite correlation. We found that the L values of the high score group were greater than those of the low score group (Table 1). It is possible that video watching drove brain connectivity from a relatively small-world structure in the resting state to another structure with serving the working state. Our result is compatible with the results of an EEG study by Micheloyannis, Pachou, Stam, Breakspear et al. (2006). The authors showed that the small-worldness of more educated participants was lower than that of less well-educated ones during a working memory task (i.e., in the working state). We interpreted the functional networks of our subjects with a higher simultaneous processing raw score as the networks of well-functioning brains. "Well-functioning" was thought to be synonymous with readiness to sacrifice small-worldness for the sake of adopting temporarily more efficient task-specific networks. The results showed that the networks of the high score group, which was the well-functioning group, had relatively longer L than other networks but that all networks had similar C (Table 1). Meanwhile, we found that the indices of the networks of the well-functioning brains were closer to the indices of a regular network during free viewing of video (Table 1). From the brain networks of a low score participant in Fig. 4(a), we could observe a large number of long distance connections. However, the long distance connections were much fewer in Fig. 4(b), which shows the network of a well-functioning brain. In the WS model, these graph indices indicate that the networks of the well-functioning brains focused on local efficiency during the free viewing of video. However, a stronger small-world structure, a structure having better balance between local efficiency and global connection, was observed in the networks of the well-functioning brains than in others in the resting state. Therefore, we presume that during the free viewing of video, the well-functioning brains were better able to drive the functional network structure towards increased efficiency in local areas.

The indices of the networks of the high score group suggested that the networks of well-functioning brains should have stronger local clustering. The graph indices of the frontal and occipital lobes indicated that the sub-networks of children with higher K-ABC scores showed better network efficiency than others did. The positive correlation of C with the higher K-ABC score, as depicted in Fig. 8(c), suggested that the sub-networks of high scoring children possessed strong local information processing ability. In addition, we found by observation of typical sub-networks (Fig. 7) that the high scoring participants' sub-networks had more local connections (Fig. 7(b)) than did those of low scoring participants (Fig. 7(a)). This suggested a strong positive correlation between local efficiency in sub-networks and cognitive performance. Therefore, during the free viewing of video, the well-functioning brain could reorganize the functional network for increased local connectivity. In such a situation, the well-functioning brain can use a network structure with relatively higher local clustering to raise the efficiency of local areas such as the frontal and occipital lobes, which are more important for the Gv ability demanded by free viewing of video.

It could be argued that our task-related sub-networks should be considered as two sub-graphs. As seen in Fig. 7, there are several connections between the two sub-networks when the degree was 8. However, we should stress that some nodes may become separated when the networks become extremely sparse, resulting in the two parts of the network becoming two separate graphs. In other previous studies, a network was considered one graph even if the graph included separated sub-graphs or separated nodes. In fact, L will be influenced by the isolation of a sub-graph, because the path lengths between isolated nodes are defined not to be infinity, but zero. However, in this study, the reason we performed the analysis on sub-networks was that we wanted to specify the relationship between K-ABC scores and local efficiency in task related brain areas. Therefore, we focused on the index of local efficiency in sub-networks, i.e., the clustering coefficient C. The sparseness of the network merely affects the clustering coefficient, because the clustering indices of isolated nodes were calculated as zero.

4.3. Compatible results in relevance studies

The negative correlation between cognitive performance and the small-world scalar obtained in this study is compatible with the observations of several other studies. Jao et al. (2013) demonstrated by fMRI analysis that the connection distance in an eyes-open condition was longer than that in an eyes-closed condition. Other studies also suggested that economical brain networks reconfigure when needed to maintain higher-cost long-range connections to support the greater requirements for information processing of the working state (Alexander-Bloch et al., 2013). Micheloyannis, Pachou, Stam, Vourkas et al. (2006) suggested that individuals with less education show an optimal small-world structure to get correct answers in a cognitive task. Here, we hypothesize that the well-functioning brain reorganizes functional connectivity to the task-related area, which results in the appearance of a network structure with higher local clustering. In another MEG study, Stam (2004) ascertained that a small-world pattern was found in low (<8 Hz) and high (>30 Hz) frequency bands, and that the frequency bands that dominated the small-worldness were those directly related to information processing. In previous similar experiments, statistically significant associations between the coherence index and cognitive performance were demonstrated in theta (6.4–7.8 Hz) and gamma (62.0–79.8 Hz) bands with statistical significance (Kikuchi et al., 2011; Kikuchi et al., 2013). Holz, Glennon, Prendergast, and Sauseng (2010) reported that theta (around 6 Hz) and gamma (around 60 Hz) bands showed phase synchronization in the parieto-occipital lobe in a visual working memory task. Therefore, we suggest the possibility that the effects of local oscillations in theta and gamma bands drive the reduction of small-worldness in the free viewing of video.

4.4. Limitations and future works

The present study suffers from several limitations. First, it is difficult to delineate more specific or precise activated areas with current methods. The graph indices calculated in this study indicate characteristics of the whole network. Characteristic of a small sub-network with a low number of vertices could easily have been submerged. However, we may consider other local graph indices on the nodal level, e.g., degree and nodal efficiency (Xue, Wang, & Tang, 2013), in future research. Second, since we did analysis at the sensor level, we were unable to acquire voxel-level information on brain organization. The K-ABC evaluated the cognitive development of children and did not allow us to analyze the influence of the anatomical development of the brain on network structure. Further studies that employ resting state MRI data will provide the anatomical dimension, although it is difficult to perform these experiments on conscious children. Third, since analyses of relevance between all of the network features of each neural rhythm and K-ABC scores could easily cause Type I statistical errors, only an analysis of the whole pass band was done. Another important reason is that recent studies suggest that cross-frequency coupling (CFC) plays a functional role in transferring information from large-scale brain networks to local cortical processing units (Canolty & Knight, 2010). A blinkered analysis of each rhythm in isolation may neglect the network connections due to CFC. Additionally, an analysis of whole bands can easily be applied to other network-feature studies.

Acknowledgments

This research is supported by the Aihara Innovative Mathematical Modelling Project, the Japan Society for the Promotion of Science (JSPS) through the "Funding Program for World-Leading Innovative R&D on Science and Technology (FIRST Program)", initiated by the Council for Science and Technology Policy (CSTP).

References

Achard, S., Salvador, R., Whitcher, B., Suckling, J., & Bullmore, E. (2006). A resilient, low-frequency, small-world human brain functional network with highly connected association cortical hubs. *The Journal of Neuroscience, 26*, 63–72.

Alexander-Bloch, A. F., Vertes, P. E., Stidd, R., Lalonde, F., Clasen, L., Rapoport, J., et al. (2013). The anatomical distance of functional connections predicts brain network topology in health and schizophrenia. *Cerebral Cortex, 23*, 127–138.

Bassett, D. S., & Bullmore, E. (2006). Small-world brain networks. *The neuroscientist, 12*, 512–523.

Bullmore, E. T., & Bassett, D. S. (2011). Brain graphs: Graphical models of the human brain connectome. *Annual Review of Clinical Psychology, 7*, 113–140.

Bullmore, E., & Sporns, O. (2012). The economy of brain network organization. *Nature Reviews Neuroscience, 13*, 336–349.

Canolty, R. T., & Knight, R. T. (2010). The functional role of cross-frequency coupling. *Trends in Cognitive Sciences, 14*, 506–515.

Cover, T. M., & Thomas, J. A. (1991). *Elements of information theory*. New York: John Wiley & Sons.

Douw, L., van Dellen, E., Baayen, J. C., Klein, M., Velis, D. N., Alpherts, W. C. J., et al. (2010). The lesioned brain: Still a small-world? *Frontiers in Human Neuroscience, 4*, 174.

Escudero, J., Hornero, R., Abásolo, D., Fernández, A., & López-Coronado, M. (2007). Artifact removal in magnetoencephalogram background activity with independent component analysis. *IEEE Transactions on Biomedical Engineering, 54*, 1965–1973.

Flanagan, D. P., Ortiz, S. O., & Alfonso, V. C. (2013). *Essentials of cross-battery assessment*. New York: John Wiley & Sons.

Holz, E. M., Glennon, M., Prendergast, K., & Sauseng, P. (2010). Theta-gamma phase synchronization during memory matching in visual working memory. *NeuroImage, 52*(1), 326–335.

Jao, T., Vértes, P. E., Alexander-Bloch, A. F., Tang, I., Yu, Y., Chen, J., et al. (2013). Volitional eyes opening perturbs brain dynamics and functional connectivity regardless of light input. *NeuroImage, 69*, 21–34.

Kaufman, A. S., & Kaufman, N. L. (1983). *Kaufman assessment battery for children: Administration and scoring manual*. Circle Pine, MN: American Guidance Service.

Kikuchi, M., Shitamichi, K., Yoshimura, Y., Ueno, S., Remijn, G. B., Hirosawa, T., et al. (2011). Lateralized theta wave connectivity and language performance in 2-to 5-year-old children. *The Journal of Neuroscience, 31*, 14984–14988.

Kikuchi, M., Yoshimura, Y., Shitamichi, K., Ueno, S., Hirosawa, T., Munesue, T., et al. (2013). A custom magnetoencephalography device reveals brain connectivity and high reading/decoding ability in children with autism. *Scientific Reports, 3*, 1139.

Langer, N., Pedroni, A., & Jancke, L. (2013). The problem of thresholding in small-world network analysis. *Plos One, 8*(1), e53199.

Liu, Y., Liang, M., Zhou, Y., He, Y., Hao, Y., Song, M., et al. (2008). Disrupted small-world networks in schizophrenia. *Brain, 131*, 945–961.

Lowe, M. J., Mock, B. J., & Sorenson, J. A. (1998). Functional connectivity in single and multislice echoplanar imaging using resting-state fluctuations. *NeuroImage, 7*, 119–132.

McGrew, K. S. (2009). CHC theory and the human cognitive abilities project: Standing on the shoulders of the giants of psychometric intelligence research. *Intelligence, 37*, 1–10.

Micheloyannis, S., Pachou, E., Stam, C. J., Breakspear, M., Bitsios, P., Vourkas, M., et al. (2006). Small-world networks and disturbed functional connectivity in schizophrenia. *Schizophrenia Research, 87*, 60–66.

Micheloyannis, S., Pachou, E., Stam, C. J., Vourkas, M., Erimaki, S., & Tsirka, V. (2006). Using graph theoretical analysis of multi channel EEG to evaluate the neural efficiency hypothesis. *Neuroscience Letters, 402*(3), 273–277.

Oostenveld, R., Fries, P., Maris, E., & Schoffelen, J. M. (2011). FieldTrip: Open source software for advanced analysis of MEG, EEG, and invasive electrophysiological data. *Computational Intelligence and Neuroscience, 2011*, 156869.

Smit, D. J. A., Stam, C. J., Posthuma, D., Boomsma, D. I., & de Geus, E. J. C. (2008). Heritability of "small-world" networks in the brain: A graph theoretical analysis of resting-state EEG functional connectivity. *Human Brain Mapping, 29*, 1368–1378.

Stam, C. J. (2004). Functional connectivity patterns of human magnetoencephalographic recordings: A 'small-world' network? *Neuroscience Letters, 355*, 25–28.

Stam, C. J., Jones, B., Nolte, G., Breakspear, M., & Scheltens, P. (2007). Small-world networks and functional connectivity in Alzheimer's disease. *Cerebral Cortex, 17*, 92–99.

Supekar, K., Musen, M., & Menon, V. (2009). Development of large-scale functional brain networks in children. *PLoS Biology, 7*, e1000157.

Tsiaras, V., Simos, P. G., Rezaie, R., Sheth, B. R., Garyfallidis, E., Castillo, E. M., et al. (2011). Extracting biomarkers of autism from MEG resting-state functional connectivity networks. *Computers in Biology and Medicine, 41*, 1166–1177.

van den Heuvel, M. P., & Hulshoff Pol, H. E. (2010). Exploring the brain network: A review on resting-state fMRI functional connectivity. *European Neuropsychopharmacology, 20*, 519–534.

van den Heuvel, M. P., Stam, C., Boersma, M., & Hulshoff Pol, H. E. (2008). Small-world and scale-free organization of voxel-based resting-state functional connectivity in the human brain. *NeuroImage, 43*, 528–539.

van den Heuvel, M. P., Stam, C. J., Kahn, R. S., & Hulshoff Pol, H. E. (2009). Efficiency of functional brain networks and intellectual performance. *The Journal of Neuroscience, 29*, 7619–7624.

Watts, D. J., & Strogatz, S. H. (1998). Collective dynamics of 'small-world'networks. *Nature, 393*, 440–442.

Xue, S. W., Wang, Y., & Tang, Y. Y. (2013). Personal and impersonal stimuli differentially engage brain networks during moral reasoning. *Brain and Cognition, 81*, 24–28.

frontiers in
HUMAN NEUROSCIENCE

ORIGINAL RESEARCH ARTICLE
published: 24 March 2014
doi: 10.3389/fnhum.2014.00170

Somatosensory evoked field in response to visuotactile stimulation in 3- to 4-year-old children

Gerard B. Remijn[1,2]*, Mitsuru Kikuchi[3], Kiyomi Shitamichi[2], Sanae Ueno[2], Yuko Yoshimura[2,4], Kikuko Nagao[3,4], Tsunehisa Tsubokawa[5], Haruyuki Kojima[6], Haruhiro Higashida[3] and Yoshio Minabe[2]

[1] International Education Center, Kyushu University, Fukuoka, Japan
[2] Department of Psychiatry and Neurobiology, Graduate School of Medical Science, Kanazawa University, Kanazawa, Japan
[3] Research Center for Child Mental Development, Kanazawa University, Kanazawa, Japan
[4] Higher Brain Functions and Autism Research, Department of Child Development, United Graduate School of Child Development, Osaka University, Osaka, Japan
[5] Department of Anesthesiology, Kanazawa University, Kanazawa, Japan
[6] Department of Psychology, Kanazawa University, Kanazawa, Japan

Edited by:
Christos Papadelis, Harvard Medical School, USA

Reviewed by:
Giancarlo Zito, 'S. Giovanni Calibita' Fatebefratelli Hospital, Italy
William C. Gaetz, The Children's Hospital of Philadelphia, USA

***Correspondence:**
Gerard B. Remijn, International Education Center, Faculty of Design, Kyushu University, Minami-ku, Shiobaru 4-9-1, Fukuoka 815-8545, Japan
e-mail: remijn@design.kyushu-u.ac.jp

A child-customized magnetoencephalography system was used to investigate somatosensory evoked field (SEF) in 3- to 4-year-old children. Three stimulus conditions were used in which the children received tactile-only stimulation to their left index finger or visuotactile stimulation. In the two visuotactile conditions, the children received tactile stimulation to their finger while they watched a video of tactile stimulation applied either to someone else's finger (the finger-touch condition) or to someone else's toe (the toe-touch condition). The latencies and source strengths of equivalent current dipoles (ECDs) over contralateral (right) somatosensory cortex were analyzed. In the preschoolers who provided valid ECDs, the stimulus conditions induced an early-latency ECD occurring between 60 and 68 ms mainly with an anterior direction. We further identified a middle-latency ECD between 97 and 104 ms, which predominantly had a posterior direction. Finally, initial evidence was found for a late-latency ECD at about 139–151 ms again more often with an anterior direction. Differences were found in the source strengths of the middle-latency ECDs among the stimulus conditions. For the paired comparisons that could be formed, ECD source strength was more pronounced in the finger-touch condition than in the tactile-only and the toe-touch conditions. Although more research is necessary to expand the data set, this suggests that visual information modulated preschool SEF. The finding that ECD source strength was higher when seen and felt touch occurred to the same body part, as compared to a different body part, might further indicate that connectivity between visual and tactile information is indexed in preschool somatosensory cortical activity, already in a somatotopic way.

Keywords: magnetoencephalography, somatosensory evoked field, somatosensory cortex, preschool child, visuotactile stimulation

INTRODUCTION

Magnetoencephalography (MEG) has become an important tool to investigate cortical activity related to sensory or cognitive processing in children of various ages (e.g., Kimura et al., 2004; Chen et al., 2010; Ciesielski et al., 2010; Gummadavelli et al., 2013). Until recently, pediatric MEG has been predominantly performed with systems designed for adult heads. For young children, such as those of preschool age, the adult MEG helmet is not ideal. Preschoolers have considerably smaller heads than adults, and since magnetic field strength decreases with increasing distance between the expected source location and the MEG sensor array (Marinkovic et al., 2004; Gaetz et al., 2008), MEG measurements can be reliably obtained only if the children are repositioned such that one side of their head is as close to the sensor surface as possible (e.g., Pihko et al., 2009). A further requirement is that the children have to minimize head and bodily movements during testing. Under natural testing conditions this is especially challenging for preschoolers aged 2- to 5-years old, since children in this age group are generally less able to suppress movements and to follow procedural instructions (for a review see Pang, 2011). While substantial MEG research has been performed with sleeping or sedated preschoolers in clinical evaluation settings (e.g., Bercovici et al., 2008; Schwartz et al., 2008; Pihko et al., 2009), few studies so far have accomplished preschool MEG measurements under natural and awake testing conditions in an adult MEG system (Fujioka and Ross, 2008; Gaetz et al., 2010).

In order to facilitate pediatric MEG, a system with a child-customized helmet has recently been developed. This helmet allows a more natural fit around the child's head and has taken away the need for repositioning the head in the dewar (e.g., Gaetz et al., 2008). To date, child-customized MEG has been successfully used with 3- to 6-year-old children to obtain auditory evoked fields to broadband noise (Johnson et al., 2010) and speech (Kikuchi et al., 2011; Ueno et al., 2012; Yoshimura et al., 2012). In the present study, we employed the system to study preschool cortical activity related to modalities other than hearing. We report a study on preschool somatosensory evoked field (SEF) in response to tactile and (multisensory) visuotactile stimuli.

Our first purpose was to expand the literature on preschool SEF. Preschool SEF in response to tactile stimulation has been reported in relatively few studies, each employing an adult MEG helmet (Gondo et al., 2001; Xiang et al., 2004; Gaetz et al., 2008; Pihko et al., 2009). Pihko et al. (2009) found that, during tactile stimulation to the finger, preschool children (1.6- to 6-years old) show a first prominent deflection in the waveform at around 50 ms (M50 component) over contralateral somatosensory cortex. The same study showed that an earlier component at around 30 ms occurs in toddlers and adults, but seldom in preschoolers. A later deflection at around 100 ms has been observed during stimulation to the thumb of toddlers (Gondo et al., 2001). This deflection, however, has not yet been reported in older preschoolers. Since still only few MEG data on preschool SEF exist, here we further investigate the deflections in the MEG waveform in 3- to 4-year-old children in response to tactile stimulation to the left index finger. The children were in natural, awake resting conditions and positioned in a child-customized MEG system.

Our second purpose was to investigate whether the deflections in the preschool waveform to tactile stimulation would already reflect modulation through visual information. In adults, it has been shown that merely watching stimulation to someone else's body part induces somatosensory activation in the viewer (e.g., Ebisch et al., 2008; Pihko et al., 2010; Meyer et al., 2011; for a review see Keysers et al., 2010). Modulatory effects of visual information containing "touch" to someone else's leg (Keysers et al., 2004), face, neck (Blakemore et al., 2005), and hand (Pihko et al., 2010) have been reported. Modulatory effects of vision have also been reported on SEF in response to tactile stimulation to an observer who watched tactile stimulation to others at the same time (Schaefer et al., 2006).

Some studies with adults have suggested that visuotactile brain responses are somatotopically organized. For example, in a study without direct tactile stimulation to the observer, Blakemore et al. (2005) found that the head area of primary somatosensory cortex was activated when observers watched touch to the face, but not to the neck. Other support for somatotopic organization has been reported in the field of action observation. Both the execution of hand and mouth actions and the mere observation of others' hand and mouth actions evoked activity in the corresponding premotor areas (Gazzola et al., 2006). Also in studies in which an observer watched stimulation to others while receiving direct tactile stimulation to the self, adult somatosensory activity seemed to reflect topographic selectivity. Motor-evoked potentials recorded from a hand region were differently modulated during observation of painful stimuli to the same hand region as compared to the foot (Avenanti et al., 2005). In preschoolers, however, modulation of somatosensory responses through visual information has not yet been explored.

To this end, we studied the effect of vision on preschool SEF with visuotactile stimuli that either concerned the same or a different body part. The stimuli comprised two visuotactile conditions (**Figure 1**). While the children received tactile stimulation to their own left index finger, they either watched mild stimulation of the left index finger (finger-touch condition) or the left toe (toe-touch condition) of someone else on a video. Besides expanding the data set on preschool SEF to unimodal tactile stimulation, i.e., without any visually presented information, we investigated whether already at the preschool age SEF undergoes modulation through vision that is somatotopically selective. If so, the adult data would suggest that SEF source strength differs between stimulation with congruent visuotactile information (finger-touch condition) and incongruent visuotactile information (toe-touch condition).

MATERIALS AND METHODS

ETHICS STATEMENT

The procedures were approved by the Ethics Committee of Kanazawa University Hospital and followed the Declaration of Helsinki. At least one parent/caregiver of each preschool participant provided written, informed consent before participation. Face-scale ratings obtained after the experiment (see below) indicated that none of the preschoolers were uncomfortable with the tactile stimulation seen on video and that felt on the finger.

PARTICIPANTS

Thirty-eight Japanese preschool children (22 females and 16 males), with an average and median age of 4 years ± 1 month, participated in the experiment. All were children from staff members of Kanazawa University Hospital or recruited from nursery schools near the hospital, in Kanazawa city, Japan. The preschoolers were right-handed, as reported by their parent(s)/caregiver(s). All had normal vision and were in normal physical health. Test results from the Japanese adaptation of the Kaufman Assessment Battery for Children (Kaufman et al., 1987) indicated that all were typically developing.

TACTILE STIMULUS AND VISUOTACTILE STIMULI

Tactile stimulation was delivered to the infant's left index finger. A 100-Hz waveform, generated by a sinusoidal oscillator (Uchida Electric, Tokyo, Japan), was used to drive a piezo-electric pulse generator attached to the finger. The repetitive pulse caused a displacement of approximately 0.5 mm of the finger tissue. Each pulse lasted 4 ms and was presented at 2 Hz, with an average time randomization of 50%, for a period of 6 min in total. The intensity of the tactile stimulation was kept constant across participants. The pulse generator and the upper part of the magic tape used to hold the child's finger over the pulse were decorated with a miniature stuffed butterfly made of soft cloth. This was wrapped gently around the participant's index finger.

Two visual stimulus conditions with a duration of 30 s were used (**Figure 1**). In the finger-touch condition, the infant watched a female left hand set against a black background (5.3 cd/m^2). The hand's index finger was alternately and repetitively touched by one of the following six pointy objects: a tine of a metal fork, a tine of a plastic yellow fork, the tip of a black pen, and the tip of a blue pencil, a red pencil, or a yellow pencil. Visual objects were changed as to avoid the theoretical chance of interference from visually evoked magnetic field induced by too much repetition of the same visual stimulus. Movement lasted 5 s for each of the six objects, together constituting a finger-touch stimulus of 30 s. The order of

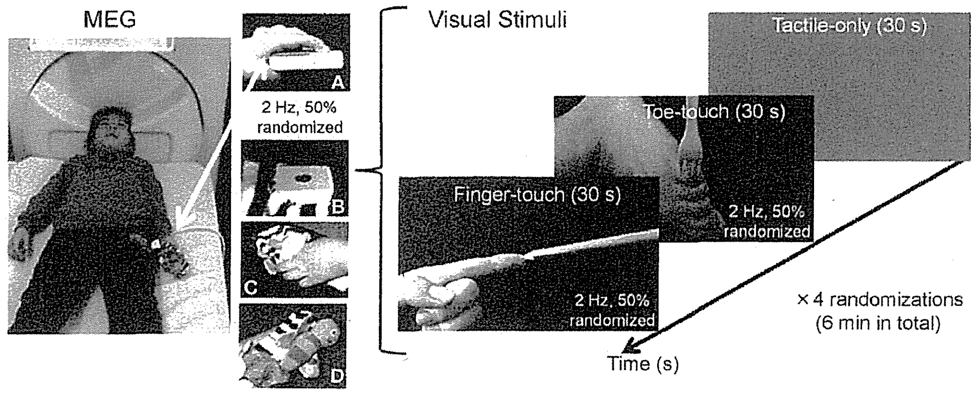

FIGURE 1 | Visuotactile stimulation used during MEG measurements of preschool somatosensory cortex. While tactile stimulation was applied to the left index finger, 3- to 4-year-old children watched tactile stimulation to someone else's left index finger (finger-touch condition) or to someone else's toe (toe-touch condition). The tactile stimulation to the children's left index finger during MEG measurements was applied through a piezo-electric stimulator **(A)**, decorated with a butterfly-like stuffed doll [**(B)** top-view; **(C)** top-view with child's finger; **(D)** side-view].

the objects was randomized for each preschool child. In the toe-touch condition, the participant watched a female left toe against the same black background. In a similar vein as in the finger-touch condition, in six randomized series of 5 s, the outside of the foot just below the little toe was touched by one of the six objects. In both the finger- and the toe-touch conditions, the objects touched the human tissue with a frequency of 2 Hz, with successive touches randomly occurring within 250–750 ms after one another. Since the felt and observed stimulation occurred to the same body part in the finger-touch condition, tactile and seen stimulation were desynchronized in order to avoid the illusion that the observed body part (e.g., the finger in the finger-touch video) was part of the observer' own body. Such a complex percept would be difficult to study reliably with preschoolers and might have been confusing to them. The two visuotactile conditions were presented with a tactile-only condition, in which the infant watched a gray screen (26.5 cd/m^2) with a white fixation cross to rest his/her eyes. The fixation cross subtended 1 × 1 deg in visual angle (112.4 cd/m^2) and was centered in the middle of the screen.

The finger-touch, toe-touch, and the tactile-only displays were generated and controlled by a personal computer (NEC VersaPro VA9), and back-projected from a display projector (Sharp PG-B10S) through four mirrors onto a 30 cm × 21 cm screen, viewed from supine position through a mirror attached to the MEG dewar. The three stimulus conditions were each repeated four times, with the order randomized for each infant. In total, 240 visual events in the finger-touch and toe-touch conditions were displayed. The total duration of the MEG measurements was 6 min. The infant was instructed to remain in a fixed bodily position and watch the screen.

STIMULI (DIS)COMFORT JUDGMENTS

Before MEG measurement, the infant was asked whether the tactile stimulation to his/her index finger was comfortable or not and told that MEG-recording could be abandoned any time he/she wanted. None of the preschoolers reported dislike or discomfort toward the piezo-electric stimulator and/or the tactile stimulation, which was reported as mild, painless stimulation above sensation threshold. None of the preschoolers opted out of the experiment. After the experiment a face-scale (Wong and Baker, 1988) was used to obtain subjective impressions of the infant's (dis)comfort with the tactile stimulation to the index finger and that seen on video. The face-scale consisted of pictures of cartoon-like faces, showing happiness (smiling) or sadness (in tears) in five intermediate steps (0–4), with "0" representing "no sensation" to "4" representing "uncomfortable sensation." When asked what their score would be if a child were to receive an injection, all preschoolers responded the maximum "4." This indicated they had understood the usage and range of the face-scale. Face-scale ratings were obtained from 35 out of 38 infants. Overall, their ratings showed that the stimuli were not discomforting. In the tactile-only condition, (dis)comfort to the finger stimulation was judged as 1.34 ± 0.26. When watching the finger-touch and the toe-touch video, this was 1.51 ± 0.23 and 1.30 ± 0.21, respectively. One-way analysis of variance (ANOVA) showed no significant difference between conditions [$F(2, 68) = 0.28$, $p = 0.75$].

MEG MEASUREMENTS AND DATA ANALYSIS

Somatosensory evoked field was recorded with a 151-channel SQUID (Super conducting Quantum Interference Device) whole-head coaxial gradiometer MEG system for children (PQ1151R, Yokogawa Electric, Kanazawa, Japan). The pick-up coils of the MEG system were 15.5 mm in diameter, the mean distance between two adjacent coils was 22 mm, and the cool-to-warm (dewar-coil) separation was 20 mm. Recordings were made in a three-layered, magnetically shielded room (Daido Steel, Nagoya, Japan), installed at the MEG-research center of Yokogawa Electric Corporation (Kanazawa, Japan). In an attempt to make the measurement environment less intimidating to the infants, the shielded room was decorated with colorful pictures of cartoon characters, familiar and liked by most Japanese preschoolers. The infant lay in a supine position on a tray-bed (Yokogawa, PQ11TA) adjusted to the height of the MEG dewar. One staff member (author YY) stayed in the shielded room to comfort the child and to encourage him/her to maintain a steady bodily position.

Magnetoencephalography data were acquired with a sampling rate of 1000 Hz and filtered with a 200-Hz low-pass filter. Time series were segmented into windows of 250 ms (−50 to 200 ms). Around 195–214 segments were averaged for each of the 151 magnetic sensors after baseline correction (−30 to −10 ms). An average of 9.7% of the segments with a noise contamination exceeding ±4 pT was excluded from the data before principal component analysis was performed for general noise reduction. At least 195 tactile events were analyzed for each condition. We determined the position of the head within the MEG dewar by measuring the magnetic fields after passing currents through coils that were attached at three locations of the head surface as the fiduciary points, with respect to the landmarks (nasion and pre-auricular points or mastoid tips). Since magnetic resonance imaging (MRI) anatomical data of the infants were not obtained, a 3-D coordinate system based on fixed MEG sensor locations was applied to calculate the equivalent current dipoles (ECDs) by using a spherical model of the volume conductor. This was fitted to the center of the fixed MEG coordinate system, after confirmation that each infant's head was located in the center of MEG dewar, by measuring the three locations of the head surface mentioned above (also see Yoshimura et al., 2012).

The single ECD model (Sarvas, 1987) was used to estimate the "center of gravity" of the current sources. We analyzed the latencies and the number of major deflection(s) in the waveform in subsequent order, and considered ECDs as valid only when (i) goodness of fit (GOF) was over 80%; (ii) the location of estimated dipoles was stable within ±5 mm of each coordinate during a period of at least 6 ms; and (iii) dipole intensities were less than 80 nA/m. As a consequence of following these criteria, there were cases in which only a single ECD in a multiple-peak waveform was considered for further analyses of source strength. ECDs for each stimulus condition were categorized according to latency with k-means cluster analysis, with the number of clusters set at three, according to the maximum number of observed major deflections in the data. Statistical analyses on the source strength were performed after taking the natural logarithm. Distribution normality was tested with the Shapiro–Wilk test and variance homogeneity was tested with Levene's test. If normality and variance homogeneity were not violated, analysis of variance (ANOVA) with independent samples was used to test the source strength between ECD latency categories within stimulus conditions, and between similar latency categories of different stimulus conditions. Paired t-tests were also performed to test source strengths between similar latency categories of different stimulus conditions, with Bonferroni correction on the alpha-level. Predominance of ECD direction within each latency category (anterior or posterior) was tested with the binomial test.

RESULTS

TACTILE-ONLY CONDITION

Figure 2 shows the three latency categories of the major deflections in the waveforms, with corresponding ECD source strengths, obtained in the tactile-only condition. The latencies of the ECDs that were in accordance with the criteria fell into categories that from here on are referred to as early-, middle-, and late-latency deflections. In the data of 17 infants, an early major deflection occurred on average at 61.65 ± 2.78 ms. In the waveform of four infants, this early peak was the only deflection observed. In eight infants, it was the first of a double-peak waveform, while in five infants, it was the first of a triple-peak waveform. In the waveforms of 11 infants, a middle-latency deflection could be observed on average at 103.82 ± 3.09 ms. In four infants, this middle-latency peak was the only deflection in the waveform. In three infants, it was the second deflection in a double-peak waveform, while in the remaining four, it was the second in a triple-peak waveform. In six infants, a late deflection in the waveform occurred on average at 150.50 ± 6.42 ms. In two infants, it was the late second in a double-peak waveform, whereas in four infants, it was the last in a triple-peak waveform.

In total, only five infants provided waveforms with double-peak deflections both of which obeyed the ECD criteria, whereas only four cases were found in which all three ECDs in a triple-peak waveform were valid. Paired comparisons between ECD source strengths over two or three latency categories would therefore suffer from a lack of power. Instead of repeated-measures ANOVA, one-way ANOVA for independent samples was performed between the source strengths of the ECDs in the three latency categories. Shapiro–Wilk tests showed no evidence for non-normality for the early-latency (df = 17, $p = 0.49$), middle-latency (df = 11, $p = 0.61$), and the late-latency ECDs (df = 6, $p = 0.47$), and homogeneity of variance was met as well (Levene statistic = 0.63, $p = 0.54$). The ANOVA showed that source strength did not significantly differ with latency category in the tactile-only condition [$F(2, 33) = 0.12, p = 0.89$]. The dipole coordinates and directions of the valid ECDs in the tactile-only condition are depicted in **Figure 3**. The tactile stimulation of the left index finger induced ECDs that were located over contralateral (right) cortex, approximately over somatosensory areas. Because of the young age of the participants, MRI-plots were not performed. Early-latency ECDs predominantly had an anterior dipole direction (14 out of 17 ECDs), rather than a posterior dipole direction. The binomial test showed that this difference was significant (two-sided, $p < 0.05$). Middle-latency ECDs were more often posteriorly directed (8 out of 11 ECDs), while late-latency ECDs were anteriorly directed in two-thirds of the cases (4 out of 6 ECDs). These trends in ECD direction in the middle-latency and late-latency category were not significant.

VISUOTACTILE CONDITIONS

The finger-touch condition induced major deflections with latency clusters that were similar as those observed in the tactile-only condition. In the finger-touch condition, an early-latency deflection occurred at 67.44 ± 1.60 ms ($n = 16$). In five children, this was the only major deflection in the waveform. In five children, it was the first of a double-peak waveform, and in six children, it was the first of a triple-peak waveform. A middle-latency deflection occurred at 101.50 ± 2.45 ms ($n = 16$). In four children, this was the only deflection in the waveform, in seven children, it was the second in a double-peak waveform, and in five children, it was the second in a triple-peak waveform. A late-latency deflection in the

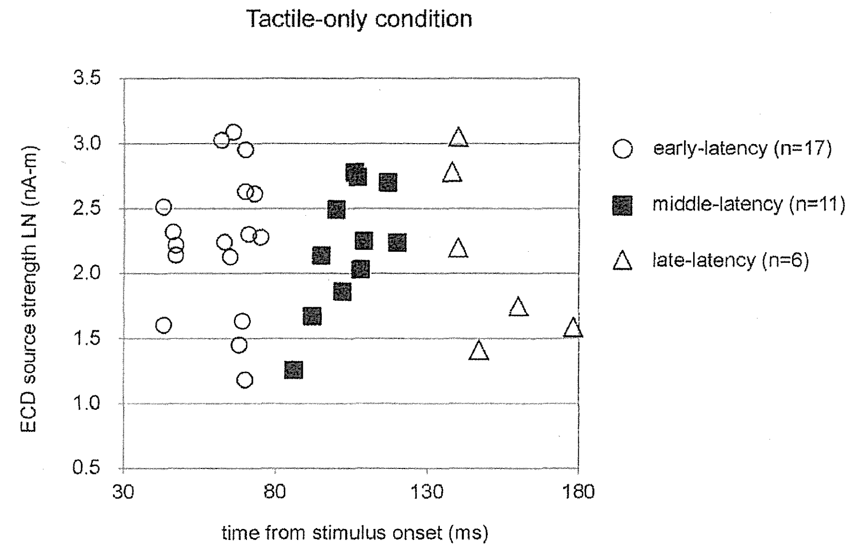

FIGURE 2 | Preschool ECD latencies and source strengths in the tactile-only condition. ECDs were obtained during piezo-electric stimulation to the left index finger of 3- to 4-year-old children. Note that the same participant could have provided data for more than one latency category, i.e., showed double-peak or triple-peak deflections in the MEG waveform that obeyed the ECD criteria. LN, natural logarithm; nA-m, nano-Ampere per meter; ms, milliseconds.

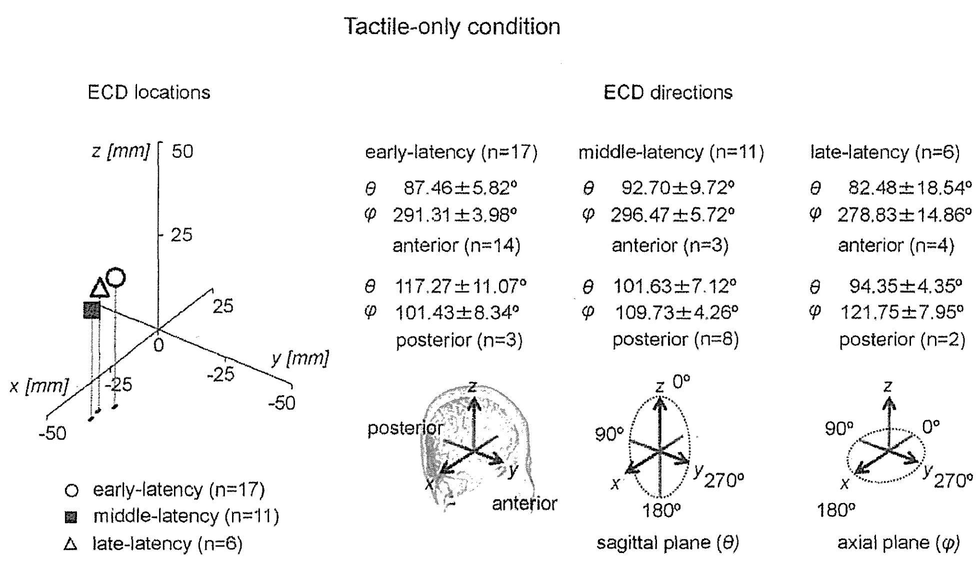

FIGURE 3 | Preschool ECD locations and directions in the tactile-only condition. ECDs were obtained during tactile stimulation to the left index finger, resulting in ECD locations in contralateral right hemisphere. Early-latency ECDs predominantly had an anterior direction. No significantly dominant direction pattern was observed for middle-latency and late-latency ECDs. Note that the same participant could have provided data for more than one category, i.e., showed double-peak or triple-peak deflections in the MEG waveform that obeyed the ECD criteria.

finger-touch condition occurred on average at 139.70 ± 3.38 ms ($n = 10$). It was the only deflection in the waveform of two children, the late second in the waveform of three children, and the third in the triple-peak waveform of five children. Only six children provided valid ECDs for both the early- and middle-latency categories, whereas only four children provided waveforms in which all ECDs in a triple-peak waveform were valid. One-way ANOVA for independent samples was therefore performed also for the finger-touch data. Shapiro–Wilk tests showed no normality violations for the early-latency (df = 16, $p = 0.26$), middle-latency (df = 16, $p = 0.06$), and the late-latency ECD groups (df = 10, $p = 0.91$). The variances among the three groups also did not differ significantly (Levene statistic = 0.42, $p = 0.66$). One-way ANOVA showed no significant difference in source strength between the latency categories in the finger-touch condition [$F(2, 41) = 0.24$, $p = 0.79$].

In the toe-touch condition an early-latency deflection occurred at 60.82 ± 2.53 ms ($n = 22$). This deflection was the only peak in the waveform of six children, the first in a double-peak waveform observed in 12 children, and the first in a triple-peak waveform of four children. A middle-latency deflection occurred on average at 97.75 ± 2.75 ms ($n = 12$). This was a single deflection in the waveform of seven children, the second in a double-peak waveform in two children, and the second in a triple-peak waveform in three children. A late-latency deflection in the toe-touch condition appeared at 139.27 ± 3.88 ms ($n = 15$). For two children, this was the only valid major deflection. For eight children, it was the second deflection in a double-peak waveform, and for five children, it was the third in a triple-peak waveform. Four children provided valid ECDs for both the early- and middle-latency categories, and only three preschoolers provided waveforms in which all ECDs in a triple-peak waveform were valid. Shapiro–Wilk tests showed no normality violations for the early-latency (df = 22, $p = 0.09$), middle-latency (df = 12, $p = 0.53$), and the late-latency ECD groups (df = 15, $p = 0.21$). The variances among the three groups also did not differ significantly (Levene statistic = 0.48, $p = 0.62$). One-way ANOVA for independent samples showed that source strength differed significantly between latency categories in the toe-touch condition [$F(2, 48) = 3.59$, $p = 0.036$]. *Post hoc* Bonferroni tests showed that for the toe-touch condition the source strength in the early-latency category was higher than that in the middle-latency category ($p = 0.034$).

The ECDs in all three latency categories in both visuotactile conditions were located at the contralateral hemisphere. Analysis of ECD directions showed that ECDs in the early-latency category had a predominantly anterior direction. In the finger-touch condition 16 out of 17 ECDs were anteriorly directed. The binomial test showed that this difference was significant (two-sided, $p < 0.01$). In the toe-touch condition, 18 out of 22 ECDs with an early-latency had an anterior direction, which was significant as well (two-sided, $p < 0.01$). ECDs in the middle-latency category were significantly more posteriorly than anteriorly directed. In the finger-touch condition, 14 out of 16 ECDs (two-sided, $p < 0.01$), and in the toe-touch condition, 10 out of 12 (two-sided, $p < 0.05$) were posteriorly located. Late-latency ECDs again were significantly more anteriorly directed. Nine out of 10 ECDs in the finger-touch condition and 12 out of 15 ECDs in the toe-touch condition had an anterior direction (two-sided, $p < 0.05$ in both cases).

COMPARISONS BETWEEN ECD SOURCE STRENGTHS IN THE TACTILE-ONLY AND THE VISUOTACTILE CONDITIONS

For each latency category, ECD source strength between the three stimulus conditions was first compared with ANOVA for independent samples. ANOVA was performed after Levene's tests showed no deviance from distribution normality in the early-latency (Levene's statistic = 0.63, $p = 0.53$), the middle-latency (Levene's statistic = 1.38, $p = 0.37$), and the late-latency (Levene's statistic = 1.16, $p = 0.33$) ECD source strengths between stimulus conditions. In the case of unpaired comparisons, source strength between the tactile-only, the finger-touch, and the toe-touch condition did not differ for the early-latency [$F(2, 54) = 0.12$, $p = 0.89$], the middle-latency [$F(2, 38) = 1.35$, $p = 0.27$], and the late-latency [$F(2, 30) = 0.18$, $p = 0.83$] categories.

Paired comparisons between ECD source strengths in similar latency categories could be made with a limited number of cases. Because few children provided data for all three latency categories in all three stimulus conditions, repeated-measures ANOVA was not performed. Instead, where possible, we performed t-tests between pairs of stimulus conditions and applied Bonferroni correction on the alpha-level. The main results are depicted in **Figures 4–6**. Paired comparisons between the tactile-only and the finger-touch condition were made for the early-latency and the middle-latency category (**Figure 4**). The late-latency category provided only four pairs and thus was not tested. Six children provided valid pairs of early-latency ECD source strengths. Shapiro–Wilk tests showed no violations of distribution normality for the early-latency tactile-only (df = 6, $p = 0.11$) and the finger-touch condition (df = 6, $p = 0.06$). Under similar variances (Levene's statistic = 0.05, $p = 0.83$), ECD source strength did not differ between the two stimulus conditions ($t = -0.52$, df = 5, $p = 0.63$). Eight children provided valid ECDs in the middle-latency category. Both the data in the tactile-only (df = 8, $p = 0.89$) and the finger-touch conditions (df = 8, $p = 0.40$) were normally distributed and showed similar variances (Levene's statistic = 0.43, $p = 0.53$). In the middle-latency category, ECD source strength in the finger-touch condition was significantly higher than in the tactile-only condition with a Bonferroni-corrected alpha-level of 0.017 for multiple paired comparisons ($t = -3.66$, df = 7, $p < 0.01$).

Paired comparisons between the tactile-only and the toe-touch conditions were also made just for the early-latency and the middle-latency category, since late-latency data were provided by only five children (**Figure 5**). Thirteen children provided valid pairs of early-latency ECD source strengths, which were normally distributed in the tactile-only condition (df = 13, $p = 0.46$) and the toe-touch condition (df = 13, $p = 0.06$). Under similar variances (Levene's statistic = 0.34, $p = 0.57$), no significant difference was found between early-latency source strengths ($t = -0.80$, df = 12, $p = 0.44$). Seven pairs could be formed with valid middle-latency ECD data. These were normally distributed in both the tactile-only condition (df = 7, $p = 0.93$) and the toe-touch condition (df = 7, $p = 0.53$) and showed no unequal variances (Levene's statistic = 2.92, $p = 0.11$). In the middle-latency category, ECD source strength in the tactile-only condition was higher than that in the toe-touch condition ($t = 3.23$, df = 6, $p = 0.018$). With the Bonferroni-corrected alpha-level ($p = 0.017$), however, this difference would strictly be not significant.

Paired comparisons between the two visuotactile conditions could be made for all three latency categories (**Figure 6**). In the early-latency category 11 paired comparisons could be made. Shapiro–Wilk tests showed no violation of source strength normality in the early-latency finger-touch (df = 11, $p = 0.34$) and

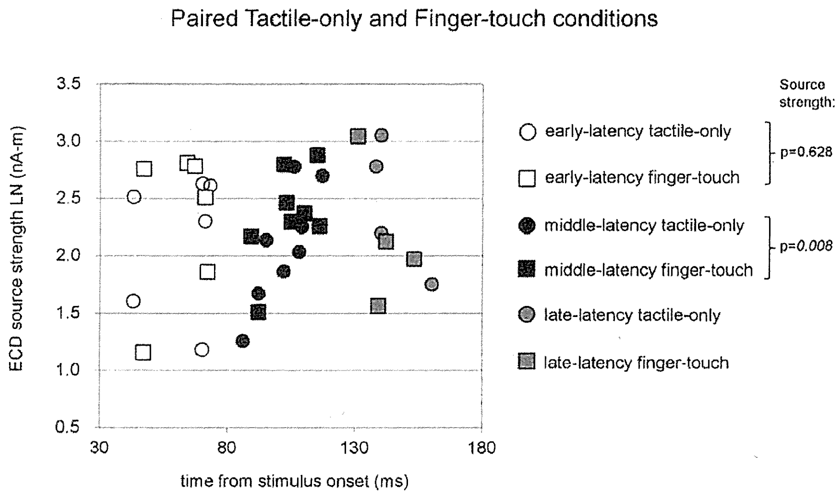

FIGURE 4 | Preschool ECD latencies and source strengths in paired tactile-only and finger-touch conditions. Circles show the tactile-only data and squares show the finger-touch data. White symbols show early-latency pairs ($n = 6$), black symbols show middle-latency pairs ($n = 8$), and gray symbols show late-latency pairs ($n = 4$). In the middle-latency category, ECD source strength was significantly higher in the finger-touch (filled black squares) than in the tactile-only condition (filled black circles). LN, natural logarithm; nA-m, nano-Ampere per meter; ms, millisecond.

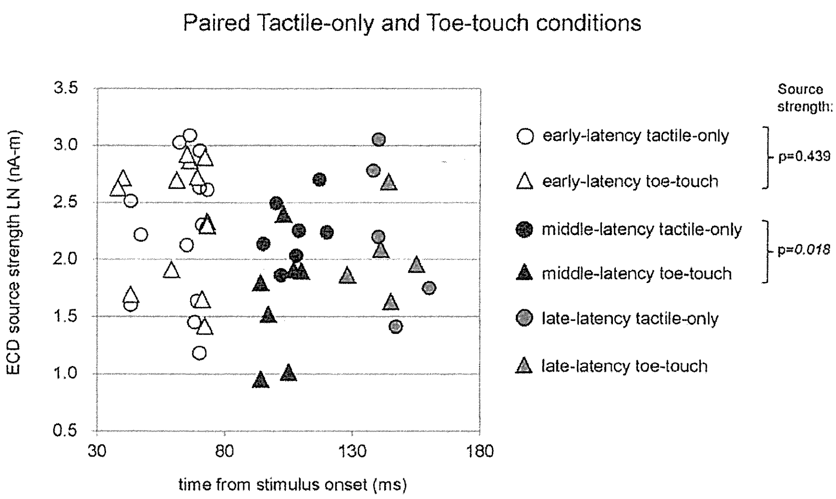

FIGURE 5 | Preschool ECD latencies and source strengths in paired tactile-only and toe-touch conditions. Circles show the tactile-only data and triangles show the toe-touch data. White symbols show early-latency pairs ($n = 13$), black symbols show middle-latency pairs ($n = 7$), and gray symbols show late-latency pairs ($n = 5$). In the middle-latency category, ECD source strength was higher in the tactile-only (filled black circles) than in the toe-touch condition (filled black triangles), but the difference strictly did not reach significance with Bonferroni correction of the alpha-level. LN, natural logarithm; nA-m, nano-Ampere per meter; ms, millisecond.

toe-touch condition ($df = 11$, $p = 0.48$). The variances in the source strengths also did not differ significantly (Levene statistic = 0.30, $p = 0.59$), and neither did the source strengths themselves ($t = 1.89$, $df = 10$, $p = 0.09$). For seven pairs in the late-latency category, source strength normality in the finger-touch ($df = 7$, 0.34) and the toe-touch ($df = 7$, 0.25) condition was not violated. Under homogeneity of variances (Levene's statistic = 0.06, $p = 0.81$), source strength in the late-latency categories did not significantly differ between the finger-touch and the toe-touch conditions ($t = 0.17$, $df = 6$, $p = 0.87$). Also for the middle-latency category seven pairs could be made. Both the source strength in the finger-touch ($df = 7$, $p = 0.24$) and toe-touch conditions ($df = 7$, $p = 0.55$) was normally distributed and variances were homogeneous (Levene's statistic = 0.33,

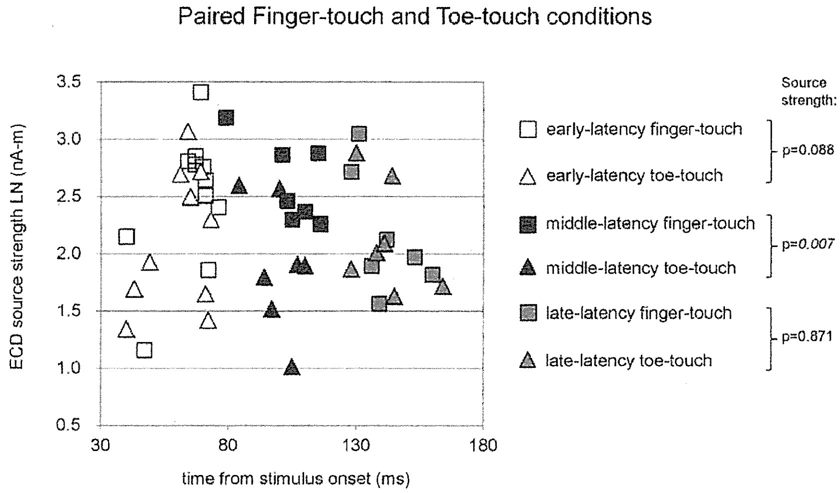

FIGURE 6 | Preschool ECD latencies and source strengths in paired finger-touch and toe-touch conditions. Squares show the finger-touch data and triangles show the toe-touch data. White symbols show early-latency pairs ($n = 11$), black symbols show middle-latency pairs ($n = 7$), and gray symbols show late-latency pairs ($n = 7$). In the middle-latency category, ECD source strength was significantly higher in the finger-touch (filled black squares) than in the toe-touch condition (filled black triangles). LN, natural logarithm; nA-m, nano-Ampere per meter; ms, millisecond.

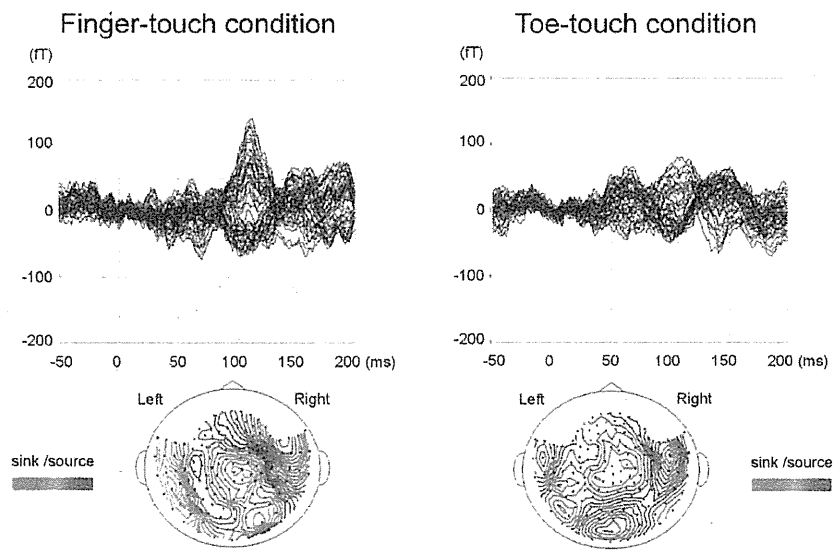

FIGURE 7 | An example of preschool SEF waveforms in the visuotactile finger-touch condition (left) and the toe-touch condition (right). The waveforms (top) and estimated ECDs (bottom) are shown for a 36-month-old girl. fT, femto-Tesla.

$p = 0.57$). The middle-latency source strength observed in the finger-touch condition was significantly higher than that in the toe-touch condition ($t = 3.97$, $df = 6$, $p < 0.01$). An example of the difference in the waveforms induced by the finger-touch and toe-touch conditions is depicted in **Figure 7**. ECD locations and directions of the paired finger- and toe-touch conditions are shown in **Figure 8**.

In summary, comparisons between ECD source strengths observed in the middle-latency categories of the three stimulus conditions showed that source strength was higher in the tactile-only condition than in the toe-touch condition. With a decreased alpha-level of 0.017 to correct for multiple comparisons, however, this difference was not significant. Even with alpha-level correction, however, middle-latency ECD source strength in

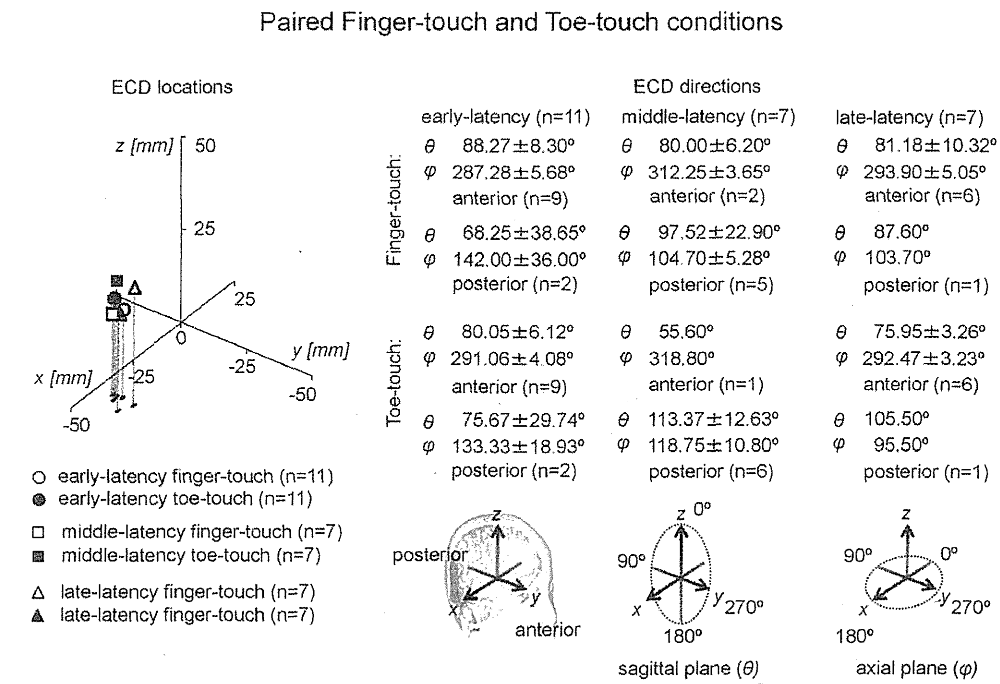

FIGURE 8 | Preschool ECD locations and directions in paired finger-touch and toe-touch conditions. ECDs were obtained during tactile stimulation to the left index finger, while the children watched a video of tactile stimulation to someone else's finger (finger-touch) or toe (toe-touch). Note that the same participant could have provided data for more than one category, i.e., showed double-peak or triple-peak deflections in the MEG waveform that obeyed the ECD criteria.

the finger-touch condition was significantly higher than in the toe-touch and the tactile-only conditions.

DISCUSSION

The present study is the first to use a child-customized MEG system to study somatosensory responses in preschool children. Besides a tactile-only condition, in which the left index finger of the preschoolers was stimulated, two visuotactile conditions were used. In one condition, the child received tactile stimulation to the index finger and at the same time watched a video of someone else being touched at the index finger. In another condition, the child received the tactile stimulation to the finger while watching a video of someone else being touched on the toe. ECD analysis showed that all three conditions induced contralateral (right-hemispheric) activity, which enabled valid dipole estimation in about 60% of the children. For all three stimulus conditions, a first valid ECD could be identified with a latency between 60 and 68 ms. This early-latency ECD had a predominantly anterior direction. The early-latency ECD strongly resembles that reported by Pihko et al. (2009), who analyzed preschool SEF with an adult MEG system. They too found a major deflection in the preschool waveform associated with an anteriorly directed dipole occurring around 60 ms (M60), but mainly in toddlers around 1 year of age in combination with an earlier component around 30 ms (M30). According to the authors, few preschoolers in the age of 1.6- to 6-years of age showed the M30, which is in accordance with the present study, but the preschoolers in the study of Pihko et al. (2009) did show a relatively prominent adult-like M50 with a posterior dipole direction. In the present study, over all conditions combined and including the cases that could not be considered in the paired comparisons, only eight preschoolers showed a posterior early-latency ECD. The average latency of this ECD was 50 ± 3.86 ms and thus indeed an M50. The vast majority (48) of the combined early-latency ECDs, however, had an anterior location with a longer latency between 60 and 68 ms. In the present study, most preschoolers thus still showed an M60. The source strengths of these early-latency ECDs did not differ between stimulus conditions. In the toe-touch condition, the early-latency ECD had a significantly more pronounced source strength than the following, middle-latency ECD.

The second, middle-latency ECD occurred on average between 97 and 104 ms in all three stimulus conditions. This latency seems to correspond with the data of Gondo et al. (2001), who reported a deflection with a latency of about 100 ms in the SEF of toddlers in response to tactile stimulation to the thumb. In the present data, the middle-latency deflection was posteriorly directed in 32 out of 39 ECDs combined over the three stimulus conditions. We further found that the source strength of the middle-latency ECD was subject to visual modulation. Although not significant with unpaired comparisons, the middle-latency ECD source strength in the finger-touch condition was significantly higher than that in the toe-touch condition in the case of paired comparisons ($n = 7$). Although paired comparisons between the source strengths observed in the visuotactile and tactile-only conditions might be inappropriate, since the tactile-only condition was a condition in which the participants could rest their eyes on the screen and arguably made less eye movements, we further found that the finger-touch condition induced a significantly higher middle-latency source strength than the tactile-only condition for $n = 8$. ECD source strength, by contrast, was higher in the tactile-only than in the toe-touch condition in the middle-latency category. With Bonferroni correction on the alpha-level, however, this difference was not significant.

The differences in middle-latency source strength between stimulus conditions suggest that visual information modulates preschool SEF. The difference between congruent (finger-touch) and incongruent (toe-touch) visuotactile stimulation might further suggest that somatotopic linkage for seen and felt touch already develops in early childhood. Out of behavioral necessity, children must learn to recognize congruent visual and tactile information that is behaviorally relevant to them as soon as possible. For example, they must quickly learn to recognize whether an object can cause comfort or pain – often by visuotactile inspection. The sparse literature related to somatotopy in child cortex concerns studies on phantom limb experiences in persons with congenitally absent limbs. In spite of being limb-deficient from birth, some of these persons experienced phantom limbs since early childhood (Poeck, 1964). The representations are likely built up through visuotactile input (Hunter et al., 2003), for example, from observation and feeling the intact limb of the self and others. Further research is necessary, though, to gain more evidence for somatotopy in the preschool brain and to clarify the mechanisms that mediate it. In the present experiment, factors such as attentional engagement toward the stimuli may have contributed to the source strength difference in the paired middle-latency ECDs obtained in the visuotactile conditions. Some MEG studies with visuotactile stimuli have implicated or specifically investigated the role of attentional engagement to the stimuli (Mima et al., 1998; Iguchi et al., 2002, 2005; Hesse et al., 2010). We can speculate, for example, that while watching the finger-touch video the children increased their attention to the stimulation to their own finger. When watching the toe-touch video, however, the children might have "ignored" the stimulation to their finger by concentrating more on their toe. This could have caused a contrast in the response strength between the toe-touch and the finger-touch conditions, assuming that the videos of stimulation to someone else's body part indeed could manipulate attentional focus of the preschooler to his/her own body part. Future research might attempt to further investigate this by quantifying the viewers' looking behavior to the video by using an eye-tracking device. Inquiries about attentional engagement to the videos and their own body part might be performed with an interview, although preschoolers might not always provide accurate and reliable answers.

Besides the early- and middle-latency ECDs, a valid ECD with a late-latency could be observed in all the stimulus conditions. The late-latency ECD occurred between 139 and 151 ms and, to our knowledge, has not been reported in preschoolers before. In the tactile-only condition, the dipole direction was anterior in four out of six children. In the two visuotactile conditions this trend was stronger: in 21 out of 25 combined ECDs the dipole direction was anteriorly directed. Significant source strength differences in the late-latency ECDs were not found between stimulus conditions.

In summary, the present study with the child-customized MEG system confirmed the occurrence of an early-latency ECD connected with tactile stimulation to the finger with a latency of about 65 ms and a predominantly anterior direction. Middle-latency ECDs were observed at around 100 ms with a predominantly posterior dipole direction. Source strength differences between paired middle-latency ECDs suggest SEF modulation through visual information in general, with congruent visuotactile information (finger-touch condition) inducing a significantly larger source strength than incongruent visuotactile information (toe-touch condition). This might reflect the development of brain functional connectivity between visual and somatosensory areas, presumably in a somatotopic way. The present preschool data further indicate the occurrence of a late-latency ECD (around 145 ms), which tended to have an anterior direction. Further research on somatosensory activity in preschool cortex is necessary to test the existence and development of (somatotopic) modulation by visual information and to expand the data in general. Also with the child-customized MEG system used here, data contamination due to motion and concentration artifacts limited the quality of the data and, hence, the number of valid ECDs that could be used for statistical comparisons.

ACKNOWLEDGMENTS

This study was supported by the Strategic Research Program for Brain Sciences of MEXT and grant 22591276 from the Japan Society for the Promotion of Science (JSPS) to Gerard B. Remijn and Mitsuru Kikuchi. The authors would like to thank everyone at Yokogawa Electric Inc., Kanazawa, Japan for technical assistance, all the participants, and the parents/caregivers of the participants. We thank Dr. Elena Pihko for informal comments on the experiment and the two reviewers for their comments on the manuscript.

REFERENCES

Avenanti, A., Bueti, D., Galati, G., and Aglioti, S. M. (2005). Transcranial magnetic stimulation highlights the sensorimotor side of empathy for pain. *Nat. Neurosci.* 8, 955–960. doi:10.1038/nn1481

Bercovici, E., Pang, E. W., Sharma, R., Mohamed, I. S., Imai, K., Fujimoto, A., et al. (2008). Somatosensory-evoked fields on magnetoencephalography for epilepsy infants younger than 4 years with total intravenous anesthesia. *Clin. Neurophysiol.* 119, 1328–1334. doi:10.1016/j.clinph.2008.02.018

Blakemore, S.-J., Bristow, D., Bird, G., Frith, C., and Ward, J. (2005). Somatosensory activations during the observation of touch and a case of vision-touch synaesthesia. *Brain* 128, 1571–1583. doi:10.1093/brain/awh500

Chen, Y., Xiang, J., Kirtman, E. G., Wang, Y., Kotecha, R., and Liu, Y. (2010). Neuromagnetic biomarkers of visuocortical development in healthy children. *Clin. Neurophysiol.* 121, 1555–1562. doi:10.1016/j.clinph.2010.03.029

Ciesielski, K. T., Ahlfors, S. P., Bedrick, E. J., Kerwin, A. A., and Hämäläinen, M. S. (2010). Top-down control of MEG alpha-band activity in children performing Categorical N-Back Task. *Neuropsychologia* 48, 3573–3579. doi:10.1016/j.neuropsychologia.2010.08.006

Ebisch, S. J., Perrucci, M. G., Ferretti, A., Del Gratta, C., Romani, G. L., and Gallese, V. (2008). The sense of touch: embodied simulation in a visuotactile mirroring mechanism for observed animate and inanimate touch. *J. Cogn. Neurosci.* 20, 1611–1623. doi:10.1162/jocn.2008.20111

Fujioka, T., and Ross, B. (2008). Auditory processing indexed by stimulus-induced alpha desynchronization in children. *Int. J. Psychophysiol.* 2, 130–140. doi:10.1016/j.ijpsycho.2007.12.004

Gaetz, W., MacDonald, M., Cheyne, D., and Snead, O. C. (2010). Neuromagnetic imaging of movement-related cortical oscillations in children and adults: age predicts post-movement beta rebound. *Neuroimage* 51, 792–807. doi:10.1016/j.neuroimage.2010.01.077

Gaetz, W., Otsubo, H., and Pang, E. W. (2008). Magnetoencephalography for clinical pediatrics: the effect of head positioning on measurement of somatosensory evoked fields. *Clin. Neurophysiol.* 119, 1923–1933. doi:10.1016/j.clinph.2008.04.291

Gazzola, V., Aziz-Zadeh, L., and Keysers, C. (2006). Empathy and the somatotopic auditory mirror system in humans. *Curr. Biol.* 16, 1824–1829. doi:10.1016/j.cub.2006.07.072

Gondo, K., Tobimatsu, S., Kira, R., Tokunaga, Y., Yamamoto, T., and Hara, T. (2001). A magentoencephalographic study on development of the somatosensory cortex in infants. *Neuroreport* 12, 3227–3231. doi:10.1097/00001756-200110290-00017

Gummadavelli, A., Wang, Y., Guo, X., Pardos, M., Chu, H., Liu, Y., et al. (2013). Spatiotemporal and frequency signatures of word recognition in the developing brain: a magnetoencephalography study. *Brain Res.* 1498, 20–32. doi:10.1016/j.brainres.2013.01.001

Hesse, M. D., Nishitani, N., Fink, G. R., Jousmäki, V., and Hari, R. (2010). Attenuation of somatosensory responses to self-produced tactile stimulation. *Cereb. Cortex* 20, 425–432. doi:10.1093/cercor/bhp110

Hunter, J. P., Katz, J., and Davis, K. D. (2003). The effect of tactile and visual sensory inputs on phantom limb awareness. *Brain* 126, 579–589. doi:10.1093/brain/awg054

Iguchi, Y., Hoshi, Y., Tanosaki, M., Taira, M., and Hashimoto, I. (2002). Selective attention regulates spatial and intensity information processing in the human primary somatosensory cortex. *Neuroreport* 13, 2335–2339. doi:10.1097/00001756-200212030-00033

Iguchi, Y., Hoshi, Y., Tanosaki, M., Taira, M., and Hashimoto, I. (2005). Attention induces reciprocal activity in the human somatosensory cortex enhancing relevant- and suppressing irrelevant inputs from fingers. *Clin. Neurophysiol.* 116, 1077–1087. doi:10.1016/j.clinph.2004.12.005

Johnson, B. W., Crain, S., Thornton, R., Tesan, G., and Read, M. (2010). Measurement of brain function in pre-school children using a custom sized whole-head MEG sensor array. *Clin. Neurophysiol.* 121, 340–349. doi:10.1016/j.clinph.2009.10.017

Kaufman, A. S., O'Neal, M. R., Avant, A. H., and Long, S. W. (1987). Introduction to the Kaufman Assessment Battery for Children (K-ABC) for pediatric neuroclinicians. *J. Child Neurol.* 2, 3–16. doi:10.1177/088307388700200102

Keysers, C., Kaas, J. H., and Gazzola, V. (2010). Somatosensation in social perception. *Nat. Rev. Neurosci.* 11, 417–428. doi:10.1038/nrn2919

Keysers, C., Wicker, B., Gazzola, V., Anton, J. L., Fogassi, L., and Gallese, V. (2004). A touching sight: SII/PV activation during the observation and experience of touch. *Neuron* 42, 335–346. doi:10.1016/S0896-6273(04)00156-4

Kikuchi, M., Shitamichi, K., Yoshimura, Y., Ueno, S., Remijn, G. B., Hirosawa, T., et al. (2011). Lateralized theta wave connectivity and language performance in 2- to 5-year-old children. *J. Neurosci.* 31, 14984–14988. doi:10.1523/JNEUROSCI.2785-11.2011

Kimura, I., Kubot, M., Hirose, H., Yumoto, M., and Sakakihara, Y. (2004). Children are sensitive to averted eyes at the earliest stage of gaze processing. *Neuroreport* 15, 1345–1348. doi:10.1097/01.wnr.0000129574.43925.59

Marinkovic, K., Cox, B., Reid, K., and Halgren, E. (2004). Head position in the MEG helmet affects the sensitivity to anterior sources. *Neurol. Clin. Neurophysiol.* 2004:30.

Meyer, K., Kaplan, J. T., Essex, R., Damasio, H., and Damasio, A. (2011). Seeing touch is correlated with content-specific activity in primary somatosensory cortex. *Cereb. Cortex* 21, 2113–2121. doi:10.1093/cercor/bhq289

Mima, T., Nagamine, T., Nakamura, K., and Shibasaki, H. (1998). Attention modulates both primary and second somatosensory cortical activities in humans: a magnetoencephalographic study. *J. Neurophysiol.* 80, 2215–2221.

Pang, E. W. (2011). Practical aspects of running developmental studies in the MEG. *Brain Topogr.* 24, 253–260. doi:10.1007/s10548-011-0175-0

Pihko, E., Nangini, C., Jousmäki, V., and Hari, R. (2010). Observing touch activates human primary somatosensory cortex. *Eur. J. Neurosci.* 31, 1836–1843. doi:10.1111/j.1460-9568.2010.07192.x

Pihko, E., Nevalainen, P., Stephen, J., Okada, Y., and Lauronen, L. (2009). Maturation of somatosensory cortical processing from birth to adulthood revealed by magnetoencephalograph. *Clin. Neurophysiol.* 120, 1552–1561. doi:10.1016/j.clinph.2009.05.028

Poeck, K. (1964). Phantoms following amputation in early childhood and in congenital absence of limbs. *Cortex* 1, 269–275. doi:10.1016/S0010-9452(64)80002-2

Sarvas, J. (1987). Basic mathematical and electromagnetic concepts of the biomagnetic inverse problem. *Phys. Med. Biol.* 32, 11–22. doi:10.1088/0031-9155/32/1/004

Schaefer, M., Flor, H., Heinze, H.-J., and Rotte, M. (2006). Dynamic modulation of the primary somatosensory cortex during seeing and feeling a touched hand. *Neuroimage* 29, 587–592. doi:10.1016/j.neuroimage.2005.07.016

Schwartz, E. S., Dlugos, D. J., Storm, P. B., Dell, J., Magee, R., Flynn, T. P., et al. (2008). Magnetoencephalography for pediatric epilepsy: how we do it. *AJNR Am. J. Neuroradiol.* 29, 832–837. doi:10.3174/ajnr.A1029

Ueno, S., Okumura, E., Remijn, G. B., Yoshimura, Y., Kikuchi, M., Shitamichi, K., et al. (2012). Spatiotemporal frequency characteristics of cerebral oscillations during the perception of fundamental frequency contour changes in one-syllable intonation. *Neurosci. Lett.* 515, 141–146. doi:10.1016/j.neulet.2012.03.031

Wong, D., and Baker, C. (1988). Pain in children: comparison of assessment scales. *Pediatr. Nurs.* 14, 9–17.

Xiang, J., Holowka, S., Qiao, H., Sun, B., and Chuang, S. (2004). Volumetric estimation of functional brain regions in small children using spatially filtered magnetoencephalography: differentiating thumb from middle finger. *Neurol. Clin. Neurophysiol.* 2004:110.

Yoshimura, Y., Kikuchi, M., Shitamichi, K., Ueno, S., Remijn, G. B., Haruta, Y., et al. (2012). Language performance and auditory evoked fields in 2- to 5-year-old children. *Eur. J. Neurosci.* 35, 644–650. doi:10.1111/j.1460-9568.2012.07998.x

Conflict of Interest Statement: The authors declare that the research was conducted in the absence of any commercial or financial relationships that could be construed as a potential conflict of interest.

Received: 05 November 2013; accepted: 07 March 2014; published online: 24 March 2014.

Citation: Remijn GB, Kikuchi M, Shitamichi K, Ueno S, Yoshimura Y, Nagao K, Tsubokawa T, Kojima H, Higashida H and Minabe Y (2014) Somatosensory evoked field in response to visuotactile stimulation in 3- to 4-year-old children. Front. Hum. Neurosci. 8:170. doi: 10.3389/fnhum.2014.00170

This article was submitted to the journal Frontiers in Human Neuroscience.

Social Cognitive and Affective Neuroscience Advance Access published April 9, 2014

doi:10.1093/scan/nsu049

Reduced long-range functional connectivity in young children with autism spectrum disorder

Mitsuru Kikuchi,[1,2] Yuko Yoshimura,[1] Hirotoshi Hiraishi,[1] Toshio Munesue,[1,2] Takanori Hashimoto,[2] Tsunehisa Tsubokawa,[3] Tsutomu Takahashi,[4] Michio Suzuki,[4] Haruhiro Higashida,[1] and Yoshio Minabe[1,2]

[1]Research Center for Child Mental Development, Kanazawa University, Kanazawa 920-8641, Japan, [2]Department of Psychiatry and Neurobiology, Graduate School of Medical Science, Kanazawa University, Kanazawa 920-8641, Japan, [3]Department of Anesthesiology, Graduate School of Medical Science, Kanazawa University, Kanazawa 920-8641, Japan, and [4]Department of Neuropsychiatry, University of Toyama, Toyama 930-0152, Japan

Autism spectrum disorder (ASD) is often described as a disorder of aberrant neural connectivity. Although it is important to study the pathophysiology of ASD in the developing cortex, the functional connectivity in the brains of young children with ASD has not been well studied. In this study, brain activity was measured non-invasively during consciousness in 50 young human children with ASD and 50 age- and gender-matched typically developing human (TD) children. We employed a custom child-sized magnetoencephalography (MEG) system in which sensors were located as close to the brain as possible for optimal recording in young children. We focused on theta band oscillations because they are thought to be involved in long-range networks associated with higher cognitive processes. The ASD group showed significantly reduced connectivity between the left-anterior and the right-posterior areas, exhibiting a decrease in the coherence of theta band (6 Hz) oscillations compared with the TD group. This reduction in coherence was significantly correlated with clinical severity in right-handed children with ASD. This is the first study to demonstrate reduced long-range functional connectivity in conscious young children with ASD using a novel MEG approach.

Keywords: autism spectrum disorder (ASD); coherence; long-range connectivity; magnetoencephalography (MEG); theta oscillation; young children

INTRODUCTION

Autism spectrum disorder (ASD) appears in infancy and early childhood, causing delays or impairments in social interaction and communication, as well as a restricted range of interests. Physiologically, in the autistic brain, reduced long-range connectivity was thought to develop in tandem with high local connectivity (Belmonte *et al.*, 2004; Courchesne and Pierce, 2005), perhaps because of widespread alterations in synapse elimination and/or formation (Sporns *et al.*, 2000). The evidence gathered with recent developments in neuroimaging methods suggests that aberrant brain connectivity reflects important aspects of brain dysfunction in ASD (Just *et al.*, 2004, 2007; Koshino *et al.*, 2005; Villalobos *et al.*, 2005; Kana *et al.*, 2006; Kleinhans *et al.*, 2008; Lee *et al.*, 2009; Monk *et al.*, 2009; Shih *et al.*, 2010; Anderson *et al.*, 2011b; Shih *et al.*, 2011; Wolff *et al.*, 2012; von dem Hagen *et al.*, 2013). To gain insight into the development of this dysfunction, it is necessary to study the pathophysiology of ASD in young children because aberrant white matter pathway development may occur during infancy (Wolff *et al.*, 2012). However, it is challenging to measure functional connectivity in young children with ASD under conscious conditions because they are not always cooperative or patient. Nonetheless, we have recently reported aberrant functional connectivity in the brain in preschool children with ASD under conscious conditions (Kikuchi *et al.*, 2013a,b). For these preliminary studies, we developed a custom child-sized magnetoencephalography (MEG) system in which the sensors are located as close to the head as possible for optimal recording, even in young children. This is a useful technique that can provide measures of cortical activity on a millisecond timescale. Other commonly used neuroimaging techniques, such as functional magnetic resonance imaging (fMRI), positron emission tomography and single-photon emission computed tomography, are limited by their poor temporal resolution relative to neural activity (i.e. brain electrical rhythms). Furthermore, MEG has advantages over these neuroimaging techniques for young children, including improved safety, fewer constraints and less environmental noise.

Coherent brain rhythms represent a core mechanism for sculpting the temporal coordination of neural activity in the brain-wide network (Wang, 2010). Rhythmic brain activity in one area is likely to be communicated to another area, generating a temporal linkage in the rhythmicity of the two structures. Given that the processing of any information involves interactions between multiple regions of the brain, the maturation of long-distance networks is likely to be crucial for cognitive development. In humans, theta oscillations have been suggested to be involved in the long-range networks associated with various cognitive processes, such as imitation (Babiloni *et al.*, 2008), top-down processing (von Stein *et al.*, 2000; von Stein and Sarnthein, 2000) and language acquisition (Kikuchi *et al.*, 2011), or with working memory and attention (Sarnthein *et al.*, 1998; Raghavachari *et al.*, 2001; Meltzer *et al.*, 2008). In this study, we hypothesized that the disturbance of long-range connectivity in young children with ASD would be reflected by a decreased coherence of theta band oscillations between distant brain areas. To verify this hypothesis, we performed coherence analysis to determine the degree of phase locking between the activities recorded by different sensors. High coherence between two MEG signals detected at distant sites (e.g. 20 cm apart) reflects phase-locked neuronal oscillations, suggesting functional integration between neural populations; in contrast, low coherence suggests independently active populations, suggesting low functional integration or functional segregation. MEG produces a reference-free signal and is therefore an ideal tool with which to compute the coherence between two distant cortical rhythms.

Due to the limits of field spreading effects, the magnetic fields generated by a single brain oscillator are rarely detected by multiple sensors when the sensors are separated by at least 20 cm (Figure 1B and C)

Received 20 September 2013; Accepted 17 March 2014

This study was supported by a Grant-in-Aid for Specially Promoted Research (Number 24000012), the Strategic Research Program for Brain Sciences from MEXT and SENSHIN Medical Research Foundation, Japan.

Correspondence should be addressed to Mitsuru Kikuchi, Research Center for Child Mental Development, Kanazawa University, 13-1 Takara-machi, Kanazawa 920-8641, Japan. E-mail: mitsuru@zc4.so-net.ne.jp

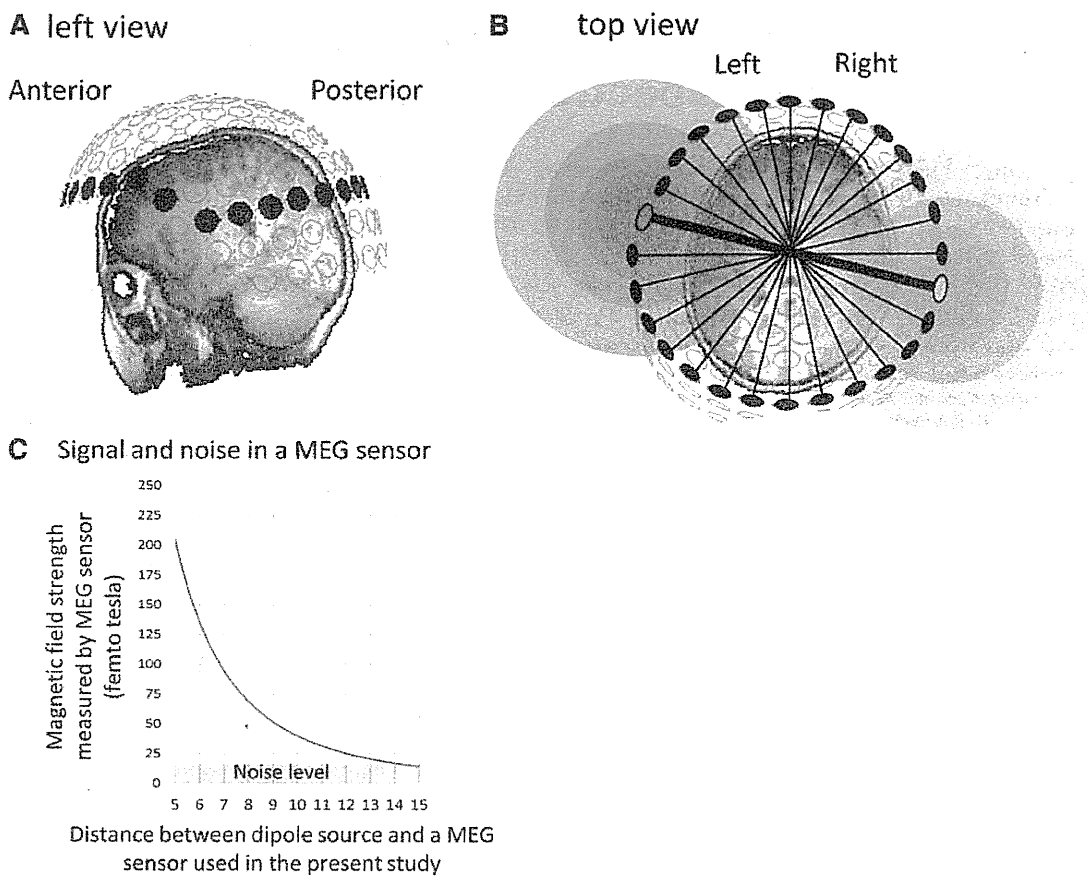

Fig. 1 Location of MEG sensors and magnetically sensitive areas. (A) Schematic of selected sensors (black closed circles) in our custom child-sized MEG system and a representative child brain (left view). (B) Schematic of 28 selected sensors (black closed circles) and 14 pairs (black solid lines) of sensors located ~20 cm apart from one another (top view). Red (or yellow)-colored areas indicate the magnetic field-sensitive areas corresponding to a red (or yellow)-colored sensor; the intensity of the color reflects the sensitivity of the area. As shown in Figure 2, a significant difference was found between this pair of sensors (indicated by a thick solid line). Note that magnetic field-sensitive areas for the two sensors (which were paired for coherence analysis) do not overlap with one another because of their distance (~20 cm). (C) Signal and noise in the MEG sensor used in this study. Magnetic field strength diminishes with distance from the source. Magnetic field strengths were measured at various distances between a dipole source and the MEG sensor. An experimental dipole source generated a 10 nAm and was measured 100 times for each distance. Signal and noise were evaluated based on the averaged data. Note the extremely poor signal-to-noise ratio at distances >10 cm.

(Srinivasan *et al.*, 2007). Our preliminary analysis with the MEG systems (Figure S1 in Supplementary Data) showed only a very small amount of brain magnetic activity that appeared to spread from a local generator to the MEG sensors, which were separated by 20 cm in our MEG system. Therefore, increased synchronization or coherence between MEG signals from sensors 20 cm apart in our MEG system is a reliable indicator of increased long-distance physiological connectivity (Figures 1B, C and S1). This spatial property of MEG sensor-level signals is thus particularly advantageous for investigating long-distance functional connectivity (Srinivasan *et al.*, 2007). However, no previous studies of ASD have used MEG sensor-level analysis (between sensors 20 cm apart). Utilizing the advantages of MEG sensors spaced 20 cm apart, this study provides the first evidence of decreased long-range connectivity in children with ASD relative to typically developing (TD) children using a simple and highly convincing method.

MATERIALS AND METHODS

Participants

The clinical group consisted of 50 children with ASD (39 males, 11 females) aged 38–92 months recruited from the Kanazawa University's Hospital and prefectural hospitals in Toyama. Children were diagnosed by a clinical psychiatrist and a clinical psychologist with more than 5 years of experience in ASD using the Autism Diagnostic Observational Schedule-Generic (ADOS) (Lord *et al.*, 1999), the Diagnostic Interview for Social and Communication Disorders (DISCO) (Wing *et al.*, 2002), the Kaufman Assessment Battery for Children (K-ABC) (Kaufman and Kaufman, 1983) and Diagnostic and Statistical Manual of Mental Disorders, Fourth Edition (DSM-IV) (American Psychiatric Association, 1994) criteria at the time of MEG and data acquisition. All ASD children included in this study fulfilled the diagnosis of childhood autism ($n = 33$), atypical autism ($n = 9$) or Asperger's syndrome ($n = 8$) with DISCO. Children with scores below the ADOS cut-offs were included in the study if they satisfied the criteria for ASD using both DSM-IV and DISCO (14 out of 50 children). The controls were 50 TD children (39 males, 11 females) aged 36–97 months with no reported behavioral or language problems. The control children were approximately age-matched to the subjects with ASD. All TD children were native Japanese and had no prior or current developmental, learning, or behavioral problems, as reported on a questionnaire completed by their parents. All participants had normal hearing ability, according to available medical records. The dominant handedness of

Table 1 Demographic characteristics of the study participants

Group	ASD children	TD children	t-test
Number of subjects	50	50	
Age (range)	66.7 months (38–92)	66.8 months (36–97)	n.s.
Gender (M/F)	39/11	39/11	
Head circumference (±s.d.)	51.2 cm (±1.4)	51.0 cm (±1.6)	n.s.
K-ABC mental processing scale (±s.d.)	96.8 (±22.5)	98.4 (±14.1)	n.s.
K-ABC achievement scale (±s.d.)	96.8 (±23.6)	100.1 (±12.8)	n.s.

n.s., no significant difference (i.e. unpaired t-test between two groups, P 14; > 14;0.05).

each participant was determined based on his or her preference for handling a spoon (TD children: right = 45, left = 4, both = 1; ASD children: right = 41, left = 2, both = 7). As shown in Table 1, the two groups were matched in chronological age and had similar K-ABC mental processing scale scores. Parents agreed to their child's participation in the study with full knowledge of the experimental nature of the research. Written informed consent was obtained prior to participation. The Ethics Committee of Kanazawa University Hospital approved the methods, and all procedures were performed in accordance with the Declaration of Helsinki.

MEG data acquisition

Recordings and offline analysis of the MEG data were performed as described in our previous studies (Kikuchi *et al.*, 2011, 2013a,b). The cognitive tasks and MEG measurements were performed on two separate days for all children. On the first day, the participants were subjected to cognitive tests and introduced to the MEG measurement environment. On the second day, participants were given instructions regarding the MEG measurement procedure. The MEG data were recorded with a multichannel SQUID (Super-conducting Quantum Interference Device) whole-head coaxial gradiometer MEG system for children (PQ 1151R; Yokogawa/KIT, Kanazawa, Japan) in a magnetically shielded room (Daido Steel, Nagoya, Japan). The MEG data were acquired at a sampling rate of 1000 Hz and filtered with a 200 Hz low-pass filter. During the MEG recording, the children lay supine on a bed and viewed a video program projected onto a screen. The position of the head within the helmet during the MEG recording was determined by measuring the magnetic fields after passing currents through coils attached at three locations on the surface of the head, which served as fiduciary marks for the bilateral mastoid processes and nasion. Prior to recording, we prepared several video programs that were entertaining for young children. The video program shown was selected by each participant. Before recording, we asked each child to confirm that he or she was content with the video program that had been selected. Offline analysis of the MEG data was performed with Brain Vision analyzer (Brain Products GmbH, Gilching, Germany) and Matlab (MathWorks, Natick, MA).

Coherence analysis

The MEG data were resampled at 500 Hz. The data were split into 2 s segments. Artifact-free segments were selected based on visual inspection. The process of eliminating contaminated data was performed blindly. At least 40 artifact-free segments (at least an 80 s period) were accepted for each subject. MEG spectra were calculated by fast Fourier transformation (FFT) with a spectral resolution of 1.0 Hz. As shown in Figure 1A and B, 14 pairs of sensors located ~20 cm apart from one another and surrounding the brain in the horizontal axis were selected prior to the offline analysis. The mean distance (±standard deviation) between each of the 14 pairs of sensors for coherence analysis was 20.3 cm (±2.9 cm). Coherences (Cross-Spectrum/Autospectrum) were calculated following a Fourier transform using the formula: Coherence $(c1, c2)(f) = |CS(c1, c2)(f)|^2/(|CS(c1, c1)(f)|\ |CS(c2, c2)(f)|)$, in conjunction with $CS(c1, c2)(f) = \Sigma c1, i(f)\ c2, i(f)^*$ (CS, Cross-Spectrum). In the second formula, totaling was carried out via segment number i. Calculation of the average also relates to segments with a fixed frequency, f, and a fixed channel, c. Using this methodology, values between 0 and 1 were obtained for each frequency and for each channel. The coherences between the 14 pairs were computed in the following six frequencies covering the theta band: 4, 5, 6, 7, 8 and 9 Hz which we are interested in.

In addition to our frequencies of interest, coherences of the following eight conventional bands were also analyzed for the same sensor pairs: delta (1.0–3.0 Hz), theta (4.0–7.0 Hz), alpha-1 (8.0–10.0 Hz), alpha-2 (11.0–12.0 Hz), beta-1 (13.0–20.0 Hz), beta-2 (21.0–30.0 Hz), gamma-1 (31.0–59.0 Hz) and gamma-2 (61.0–80.0 Hz).

To investigate the range of alpha rhythms in the ASD and TD participants, MEG spectra were re-calculated using a FFT with a spectral resolution of 0.5 Hz. The absolute power was normalized with the total power (1–80 Hz) and the averages of over 151 sensors, and alpha peak frequencies were recorded for both groups.

Statistical analysis

Unpaired t-tests were performed to compare the ASD and TD groups. To compensate for the multiple comparisons between the 14 long-distance sensor pairs and for six frequencies of interest, the alpha level was adjusted to 0.05/84 = 0.00060. As a complementary approach, an alpha level of 0.05 was also employed, with the risk of increasing the chance of Type I error, to explore the differences in physiological measures between the ASD and TD groups.

If there was a significant difference in the coherence between two groups even after the alpha level was adjusted, a Pearson's correlation was used to find significant correlations between the coherence and clinical severity as scored using ADOS (i.e. the sum of the communication domain and social interaction domain scores). The significance level was set at $P < 0.05$ for this correlation analysis.

For the complementary analysis with the eight conventional bands (i.e. delta–gamma bands), unpaired t-tests were performed to compare the ASD and TD groups. Similar to the analysis within the theta band, the significance level was set to $P < 0.00060$.

Alpha peak frequencies were also compared between the ASD and TD groups using unpaired t-tests, for which the significance level was set to $P < 0.05$.

RESULTS

Coherence in the ASD and TD groups

As shown in Figure 2, after Bonferroni correction, unpaired t-tests identified one pair of sensors (left-anterior and right-posterior areas) for which the ADS group showed significantly lower coherence in 6 Hz oscillations compared with TD children ($t = 4.38$, $P < 0.0001$). When we employed an alpha level of 0.05, with the increased risk of Type I errors, some significant differences arose between two groups. In the 5-, 6-, 7- and 9 Hz oscillations, there were eight pairs of additional sensors for which significantly lower coherence was found for the ASD group compared with the TD group ($P < 0.05$). As shown in Figure 2, six of the nine significant pairs seem to reflect connectivity between anterior and posterior brain areas, whereas three of the nine significant pairs seem to reflect connectivity between left-anterior and right-posterior brain areas. The ASD group did not show significantly higher coherence than the TD group for any pair of sensors at any frequency.

With regard to the absolute power values, which are shown in Table S1 of the Supplementary Data, there were no significant

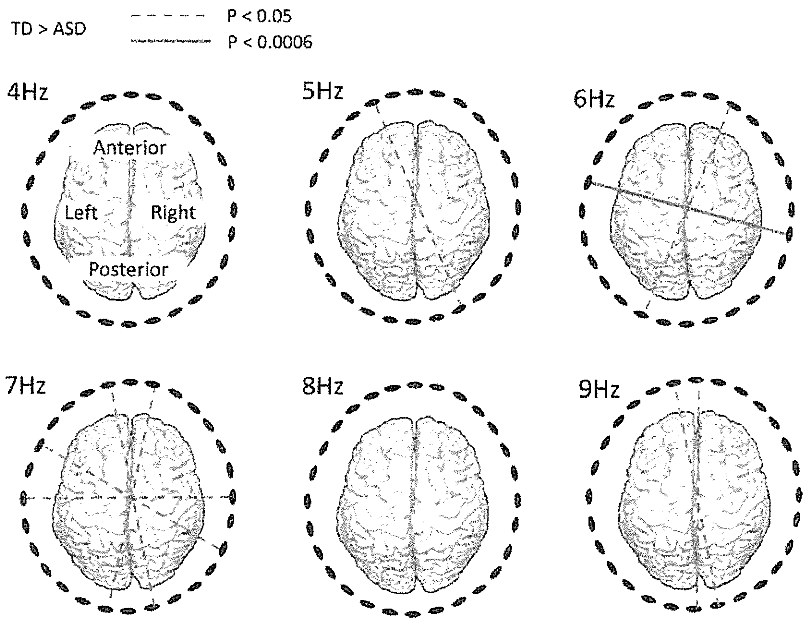

Fig. 2 Results of the unpaired t-tests comparing coherence values from children with ASD ($n = 50$) and TD ($n = 50$) children for each frequency oscillation in the theta band. The solid red line ($P < 0.0006$) and the broken red lines ($P < 0.05$) indicate the pairs of sensors for which reduced coherence was observed in children with ASD compared with TD children. Note that, in the 6 Hz oscillation, there was one pair of sensors (indicated by a solid red line between the left-anterior and the right-posterior areas) for which significantly reduced coherence was found in ASD children compared with TD children, even after Bonferroni correction ($t = 4.38$, $P < 0.0001$). In the 5-, 6-, 7- and 9 Hz oscillations, eight pairs of sensors (broken line) showed a tendency toward decreased coherence in ASD children compared with TD children ($P < 0.05$). No pairs of sensors showed significantly increased coherence in children with ASD compared with TD children at any frequency ($P > 0.05$).

differences between the TD and ASD groups for any sensor, even using a non-conservative alpha level of 0.05 (i.e. $|t\text{-value}| = 1.98$).

With regard to the coherences of the eight conventional delta–gamma bands, which are shown in Figure S2 of the Supplementary Data, there were no significant differences for any sensor using a conservative alpha level of 0.00060. Using an alpha level of 0.05, six pairs of sensors showed a tendency toward decreased or increased coherence in ASD children compared with TD children. However, with 112 multiple comparisons, six pairs are approximately a number of pairs that would be expected to reach statistical significance by chance alone.

Relation between coherence and symptom

Pearson's correlation analysis revealed a tendency for negative correlation between coherence in the 6 Hz oscillation (left-anterior and right-posterior in the 6 Hz oscillation) and ADOS score ($r = -0.28$, $P = 0.051$). When we divided the group based on handedness, as shown in Figure 3B, this correlation was found to be significant in right-handed children with ASD ($r = -0.37$, $P = 0.016$). To evaluate the existence of possible gender, intelligence level and/or age effects on the significance of the relationship found in right-handed children with ASD, we used multiple linear regression to predict this coherence value using ADOS score, K-ABC mental processing quotient, age and gender as predictors (i.e. four independent variables). The significance level was set at $P < 0.05$. In the multiple regression model, the ADOS score remained a significant predictor of the coherence ($n = 41$, $\beta = -0.35$, $P = 0.028$), whereas K-ABC mental processing quotient ($n = 41$, $\beta = -0.06$, $P > 0.05$), age ($n = 41$, $\beta = 0.00$, $P > 0.05$) and gender ($n = 41$, $\beta = -0.24$, $P > 0.05$) did not reach statistical significance.

Alpha peak frequencies in the ASD and TD groups

As shown in Figure S3 of the Supplementary Data, the MEG spectra demonstrated that alpha peak frequencies were ~9.0 Hz in both groups. Out of the 50 children in the two groups, a clear peak on the FFT spectrum was detected in 41 TD and 48 ASD children. The mean measurable alpha peak frequencies were 8.8 (range: 7.5–10.0 Hz) for TD children and 9.1 (range: 7.5–10.5 Hz) for ASD children. However, an unpaired t-test failed to demonstrate a significant difference between the groups ($t = 1.20$, $P > 0.05$).

A complementary approach (coherence from the full set of MEG sensors)

A complementary analysis involved an additional analysis of coherence using the full set of MEG sensors, which included 151 channels. The sensor that corresponded to the left frontal area, in which robust significant differences were observed in the coherence analysis at 6 Hz, was used as a seed sensor. The coherence values between this seed sensor and the remaining 150 sensors at 6 Hz were calculated, and an unpaired t-test was used to compare these values between the ASD and TD groups. As shown in Figure 4, the unpaired t-test demonstrated significantly lower coherence for the 6 Hz oscillation between the left frontal sensor (the seed sensor) and a cluster of sensors in the right posterior area (located more than 20 cm apart) in children with ASD compared with TD children.

DISCUSSION

Herein, we provide credible evidence indicating that there is reduced connectivity between the left-anterior and right-posterior brain areas in ASD children (3–7 years old), as demonstrated by 6 Hz oscillation patterns (Figures 3A and 4). This reduced connectivity was

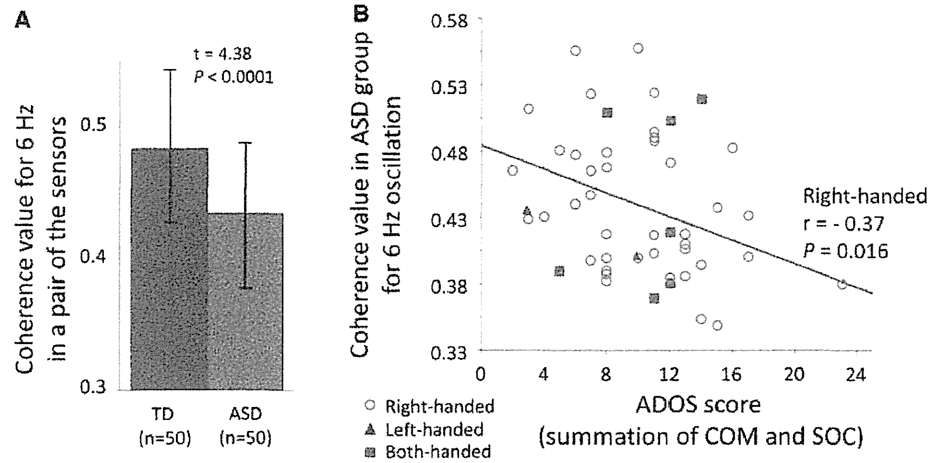

Fig. 3 Reduced coherence in children with ASD and its correlation with clinical severalty. (A) Coherence values of the 6 Hz oscillation in the pair of sensors (left-anterior and right-posterior area) that exhibited significantly reduced coherence in ASD children compared with TD children, even after Bonferroni correction ($t = 4.38$, $P < 0.0001$). The error bars represent 1 s.d. (B) Scatter plot of coherence values for 6 Hz oscillations between the left-anterior and the right-posterior areas in ASD children and the sum of the ADOS COM and SOC scores in children with ASD. In right-handed children with ASD ($n = 41$), these values tended to be negatively correlated ($r = -0.37$, $P = 0.016$); this correlation weakened when all children with ASD were included ($n = 50$, $r = -0.28$, $P = 0.051$). Open red circle, right-handed children with ASD ($n = 41$); blue triangle, left-handed children with ASD ($n = 2$); green square, both-handed children with ASD ($n = 7$); solid red line, regression line for right-handed children with ASD. COM, communication domain; SOC, social interaction domain.

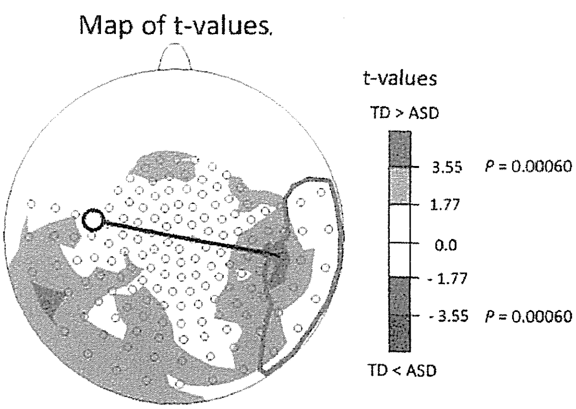

Fig. 4 Map of *t*-values between ASD and TD children for coherence values for the 6 Hz oscillation that were calculated with a seed sensor (yellow circle) and other sensors. The area surrounded by a green line represents the region in which the distance from the seed sensor (yellow circle) is >20 cm. In ASD children, a cluster of sensors showed a robust significant decrease (i.e. $P < 0.00060$) of 6 Hz coherence in the long-distance area. The black solid line indicates the sensor pair in which a robust significant difference was demonstrated in the first analysis for the 6 Hz oscillation (Figure 2).

significantly correlated with higher symptom severity, as scored using ADOS, in right-handed children with ASD (Figure 3B).

Our results are compatible with several recent reports of reduced brain hemodynamic synchronization in young children, adolescents and adults with ASD (Cherkassky *et al.*, 2006; Kennedy and Courchesne, 2008; Monk *et al.*, 2009; Anderson *et al.*, 2011a; Dinstein *et al.*, 2011). Most importantly, two recent studies reported significantly decreased inter-hemispheric synchronization in multiple cortical areas in toddlers with ASD (Dinstein *et al.*, 2011) and in adolescents and adults with ASD (Anderson *et al.*, 2011a). One explanation for these findings is that the reduced inter-hemispheric synchronization that is present in young children with ASD persists into adulthood. Structural imaging has also demonstrated abnormalities in inter-hemispheric long-range white matter pathways. Corpus callosum volume has been used as an index of inter-hemispheric connectivity, and a reduced corpus callosum volume is one of the most replicated structural findings in ASD (Manes *et al.*, 1999; Hardan *et al.*, 2000; Vidal *et al.*, 2006; Alexander *et al.*, 2007; Stanfield *et al.*, 2008; Keary *et al.*, 2009). These findings in ASD have been shown to be correlated with intra-hemispheric functional underconnectivity (Just *et al.*, 2007; Mason *et al.*, 2008). A diffusion tensor analysis of the corpus callosum also demonstrated significant microstructural differences between ASD and control groups in fractional anisotropy, mean diffusivity and radial diffusivity (Alexander *et al.*, 2007; Keller *et al.*, 2007; Brito *et al.*, 2009; Wolff *et al.*, 2012). Most importantly, one recent study demonstrated that in infants with ASD compared with infants without ASD, development for most measurable fiber tracts (i.e. not only the corpus callosum) was characterized by higher fractional anisotropy values at 6 months followed by slower changes over time; by 24 months of age, the ASD group had lower values (Wolff *et al.*, 2012). This study is consistent with these structural and functional connectivity studies by suggesting that in ASD children (3–7 years old), there is reduced inter-hemispheric connectivity in the 6 Hz oscillation, and this reduced connectivity is correlated with symptom severity.

When we accepted an alpha level of 0.05, at the risk of increased Type I errors, certain significant differences arose between the two groups. As shown in Figure 2, six of the nine pairs of sensors that showed significantly decreased coherence in the ASD group were oriented in the anteroposterior direction. These results suggested that there was reduced connectivity between the frontal lobes and posterior brain areas in young children with ASD, results that are consistent with a putative model of pathophysiology in which the connectivity between the frontal cortex and other systems is poorly synchronized, weakly responsive, and information impoverished in ASD (Courchesne and Pierce, 2005). Previous neuroimaging studies using fMRI supported this hypothesis in adult subjects with ASD (Villalobos *et al.*, 2005; Kana *et al.*, 2006; Just *et al.*, 2007). Our results also support this putative model of pathophysiology (i.e. lower functional connectivity between anterior and posterior areas) in preschool children with ASD.

For both electroencephalography (EEG) and MEG sensor-level signals, it is difficult to demonstrate short-range brain physiological connectivity (e.g. <10 cm) with high reliability and confidence because volume conduction effects or magnetic field spreading effects can distort the results such that they are unable to provide credible information about functional connectivity. However, long-range brain connectivity can be evaluated accurately with MEG using sensors located 20 cm apart because of the limit of the field spreading effect (Figures 1B, C and S1) (Srinivasan *et al.*, 2007); this evaluation remains difficult with a scalp-based EEG method. In addition, MEG produces a reference-free signal and is therefore an ideal tool to compute coherence between two distant cortical rhythms. In contrast, in EEG coherence analysis, an improper reference can distort the results and interfere with their interpretation (Hu *et al.*, 2010). Utilizing the advantages of signals from MEG sensors spaced 20 cm apart, this is the first study to demonstrate that reduced long-range brain connectivity is one of the hallmarks of ASD at a very young age.

In our previous study, using widely distributed MEG sensors, we were unable to demonstrate decreased theta band coherence in the ASD group compared with the TD group (Kikuchi *et al.*, 2013a,b). Rather, we reported higher coherence in the gamma-band oscillations of the temporal and occipital areas in the ASD group (Kikuchi *et al.*, 2013b). In these studies, the distance between the temporal and occipital sensors was <15 cm, and therefore we could not exclude the possibility that higher short-range connectivity in a gyrus located between the temporal and occipital areas yielded a relatively coherent oscillation that spread to both sensors (<15 cm apart). In this study, utilizing the advantages of signals from MEG sensors 20 cm apart, we were able to minimize any spurious connectivity caused by the field spreading effect.

In this study, we identified a robust significant difference in the 6 Hz oscillation in one pair of sensors (i.e. the left-anterior and right-posterior areas). In a previous EEG study using a power analysis, the functional theta rhythm in preschool children during attention to social stimulation was reported (Orekhova *et al.*, 2006). The functional theta rhythms ranged from 4 to 8 Hz, with a peak frequency of ~6 Hz in preschool children (Orekhova *et al.*, 2006). Therefore, our results (i.e. aberrant brain functional connectivity via theta oscillation) may reflect aberrant functional theta oscillations that are relevant to social stimuli in ASD children. As shown in Figure S4, the coherence values for the 5 and 7 Hz oscillations tended to be reduced in ASD children compared with TD children, with a similar significant effect found for 6 Hz oscillation. Although aberrant brain connectivity relevant to social stimuli in ASD children may be distributed across a more wide frequency range (e.g. 4–8 Hz), a significant difference was only found for the 6 Hz oscillation. One possible explanation for this restricted result is the confounding factor of the alpha rhythm at 7, 8 and 9 Hz. As shown in Figure S3, the theta and alpha frequency bands partly overlapped at 7 and 8 Hz in this study. Although the theta activity in preschool children is distinct from the alpha activity, the upper boundary of the theta frequency band is close to the alpha peak frequency for this age. Thus, the theta and alpha bands may overlap due to age-related and inter-individual variability. Furthermore, one cannot exclude the possibility that the theta and alpha frequency bands partly overlap in the same subject.

This study has some limitations. First, there is a possibility that the differences in measured coherence may relate to the different spatiotemporal properties of the video stimuli during the periods corresponding to the selected artifact-free segments. In addition, we did not evaluate the degree to which the subjects focused on the TV program that they chose. Further studies that employ attention-controlled conditions will provide more reliable evidence, although these conditions will likely be difficult to achieve in conscious preschool-aged young children. Second, to ensure a simple and credible analysis using raw MEG data, we were limited to 14 pairs of sensors located ~20 cm apart from one another. In exchange for a credible connectivity analysis with the lowest possible magnetic field spreading effect, we lost the flexibility to choose various pairs of the MEG sensors (e.g. we could not choose any pair of sensors, such as that between anterior and temporal areas in the same hemisphere, as the distance between them is <15 cm). Third, coherence between a pair of sensors can increase not only because two distinct sources provide activity that has become more phase-locked but also because a single source generates a signal that reaches both sensors. In our study, to reduce the latter possibility, we used a sparse alignment of MEG sensors (e.g. the distance between the sensors was at least 20 cm); however, we cannot deny the latter possibility completely. Fourth, given that young children were examined in this study, we were unable to obtain structural brain information onto which we could superimpose the coordinate systems of the source-estimated MEG signals, as described in a previous study of adults with ASD (Honaga *et al.*, 2010). This limitation was encountered because it is difficult to perform additional MRI when studying young children. Therefore, we performed a sensor-level analysis. However, future studies using child-friendly, open-type MRI devices and source-space imaginary coherence analysis with beamforming methods (Sekihara *et al.*, 2011), which have become a popular method of estimating functional connectivity based on MEG/EEG, will enable us to investigate the source level brain network in young children under conscious conditions. Fifth, a majority of the children with ASD in this study were high-functioning subjects who were able to remain stationary during the MEG measurements; therefore, the findings may not apply to children with 'Kanner's Autism' who have difficulty remaining stationary.

CONCLUSIONS

In summary, the ASD group showed significantly reduced connectivity between the left-anterior and the right-posterior areas, exhibiting a decrease in the coherence of theta band (6 Hz) oscillations compared with the TD group. This reduction in coherence was significantly correlated with clinical severity in right-handed children with ASD. This is the first study to demonstrate reduced long-range functional connectivity in conscious young children with ASD using a novel and credible MEG approach.

Conflicts of Interest

The authors declare that they have no conflicts of interest.

SUPPLEMENTARY DATA

Supplementary data are available at *SCAN* online

REFERENCES

Alexander, A.L., Lee, J.E., Lazar, M., et al. (2007). Diffusion tensor imaging of the corpus callosum in autism. *Neuroimage, 34*, 61–73.

American Psychiatric Association (editor). (1994). *Diagnostic and Statistical Manual of Mental Disorders (DSM-IV)*. Washington, DC: American Psychiatric Association.

Anderson, J.S., Druzgal, T.J., Froehlich, A., et al. (2011a). Decreased interhemispheric functional connectivity in autism. *Cerebral Cortex, 21*, 1134–46.

Anderson, J.S., Nielsen, J.A., Froehlich, A.L., et al. (2011b). Functional connectivity magnetic resonance imaging classification of autism. *Brain, 134*, 3739–51.

Babiloni, C., Vecchio, F., Bares, M., et al. (2008). Functional coupling between anterior prefrontal cortex (BA10) and hand muscle contraction during intentional and imitative motor acts. *Neuroimage, 39*, 1314–23.

Belmonte, M.K., Allen, G., Beckel-Mitchener, A., Boulanger, L.M., Carper, R.A., Webb, S.J. (2004). Autism and abnormal development of brain connectivity. *The Journal of Neuroscience, 24*, 9228–31.

Brito, A.R., Vasconcelos, M.M., Domingues, R.C., et al. (2009). Diffusion tensor imaging findings in school-aged autistic children. *Journal of Neuroimaging, 19*, 337–43.

Cherkassky, V.L., Kana, R.K., Keller, T.A., Just, M.A. (2006). Functional connectivity in a baseline resting-state network in autism. *Neuroreport, 17*, 1687–90.

Courchesne, E., Pierce, K. (2005). Why the frontal cortex in autism might be talking only to itself: local over-connectivity but long-distance disconnection. *Current Opinion in Neurobiology, 15*, 225–30.

Dinstein, I., Pierce, K., Eyler, L., et al. (2011). Disrupted neural synchronization in toddlers with autism. *Neuron, 70*, 1218–25.

Hardan, A.Y., Minshew, N.J., Keshavan, M.S. (2000). Corpus callosum size in autism. *Neurology, 55*, 1033–6.

Honaga, E., Ishii, R., Kurimoto, R., et al. (2010). Post-movement beta rebound abnormality as indicator of mirror neuron system dysfunction in autistic spectrum disorder: an MEG study. *Neuroscience Letters, 478*, 141–5.

Hu, S., Stead, M., Dai, Q., Worrell, G.A. (2010). On the recording reference contribution to EEG correlation, phase synchrony, and coherence. *IEEE Transactions on Systems, Man, and Cybernetics. Part B, Cybernetics, 40*, 1294–304.

Just, M.A., Cherkassky, V.L., Keller, T.A., Kana, R.K., Minshew, N.J. (2007). Functional and anatomical cortical underconnectivity in autism: evidence from an FMRI study of an executive function task and corpus callosum morphometry. *Cerebral Cortex, 17*, 951–61.

Just, M.A., Cherkassky, V.L., Keller, T.A., Minshew, N.J. (2004). Cortical activation and synchronization during sentence comprehension in high-functioning autism: evidence of underconnectivity. *Brain, 127*, 1811–21.

Kana, R.K., Keller, T.A., Cherkassky, V.L., Minshew, N.J., Just, M.A. (2006). Sentence comprehension in autism: thinking in pictures with decreased functional connectivity. *Brain, 129*, 2484–93.

Kaufman, A., Kaufman, N. (1983). Kaufman Assessment Battery for Children: Administration and Scoring Manual. *Circle Pines*. MN: American Guidance Service.

Keary, C.J., Minshew, N.J., Bansal, R., et al. (2009). Corpus callosum volume and neurocognition in autism. *Journal of Autism and Developmental Disorders, 39*, 834–41.

Keller, T.A., Kana, R.K., Just, M.A. (2007). A developmental study of the structural integrity of white matter in autism. *Neuroreport, 18*, 23–7.

Kennedy, D.P., Courchesne, E. (2008). The intrinsic functional organization of the brain is altered in autism. *Neuroimage, 39*, 1877–85.

Kikuchi, M., Shitamichi, K., Yoshimura, Y., et al. (2013a). Altered brain connectivity in 3- to 7-year-old children with autism spectrum disorder. *NeuroImage: Clinical, 2*, 394–401.

Kikuchi, M., Shitamichi, K., Yoshimura, Y., et al. (2011). Lateralized theta wave connectivity and language performance in 2- to 5-year-old children. *The Journal of Neuroscience, 31*, 14984–8.

Kikuchi, M., Yoshimura, Y., Shitamichi, K., et al. (2013b). A custom magnetoencephalography device reveals brain connectivity and high reading/decoding ability in children with autism. *Scientific Reports, 3*, 1139.

Kleinhans, N.M., Richards, T., Sterling, L., et al. (2008). Abnormal functional connectivity in autism spectrum disorders during face processing. *Brain, 131*, 1000–12.

Koshino, H., Carpenter, P.A., Minshew, N.J., Cherkassky, V.L., Keller, T.A., Just, M.A. (2005). Functional connectivity in an fMRI working memory task in high-functioning autism. *Neuroimage, 24*, 810–21.

Lee, P.S., Yerys, B.E., Della Rosa, A., et al. (2009). Functional connectivity of the inferior frontal cortex changes with age in children with autism spectrum disorders: a fcMRI study of response inhibition. *Cerebral Cortex, 19*, 1787–94.

Lord, C., Rutter, M., DiLavore, P., Risi, S. (1999). *Autism Diagnostic Observation Schedule*. Los Angeles, CA: Western Psychological Services.

Manes, F., Piven, J., Vrancic, D., Nanclares, V., Plebst, C., Starkstein, S.E. (1999). An MRI study of the corpus callosum and cerebellum in mentally retarded autistic individuals. *The Journal of Neuropsychiatry and Clinical Neurosciences, 11*, 470–4.

Mason, R.A., Williams, D.L., Kana, R.K., Minshew, N., Just, M.A. (2008). Theory of Mind disruption and recruitment of the right hemisphere during narrative comprehension in autism. *Neuropsychologia, 46*, 269–80.

Meltzer, J.A., Zaveri, H.P., Goncharova, II, et al. (2008). Effects of working memory load on oscillatory power in human intracranial EEG. *Cerebral Cortex, 18*, 1843–55.

Monk, C.S., Peltier, S.J., Wiggins, J.L., et al. (2009). Abnormalities of intrinsic functional connectivity in autism spectrum disorders. *Neuroimage, 47*, 764–72.

Orekhova, E.V., Stroganova, T.A., Posikera, I.N., Elam, M. (2006). EEG theta rhythm in infants and preschool children. *Clinical Neurophysiology, 117*, 1047–62.

Raghavachari, S., Kahana, M.J., Rizzuto, D.S., et al. (2001). Gating of human theta oscillations by a working memory task. *The Journal of Neuroscience, 21*, 3175–83.

Sarnthein, J., Petsche, H., Rappelsberger, P., Shaw, G.L., von Stein, A. (1998). Synchronization between prefrontal and posterior association cortex during human working memory. *Proceedings of the National Academy of Sciences of the United States of America, 95*, 7092–6.

Sekihara, K., Owen, J.P., Trisno, S., Nagarajan, S.S. (2011). Removal of spurious coherence in MEG source-space coherence analysis. *IEEE Transactions on Bio-Medical Engineering, 58*, 3121–9.

Shih, P., Keehn, B., Oram, J.K., Leyden, K.M., Keown, C.L., Muller, R.A. (2011). Functional differentiation of posterior superior temporal sulcus in autism: a functional connectivity magnetic resonance imaging study. *Biological Psychiatry, 70*, 270–7.

Shih, P., Shen, M., Ottl, B., Keehn, B., Gaffrey, M.S., Muller, R.A. (2010). Atypical network connectivity for imitation in autism spectrum disorder. *Neuropsychologia, 48*, 2931–9.

Sporns, O., Tononi, G., Edelman, G.M. (2000). Theoretical neuroanatomy: relating anatomical and functional connectivity in graphs and cortical connection matrices. *Cerebral Cortex, 10*, 127–41.

Srinivasan, R., Winter, W.R., Ding, J., Nunez, P.L. (2007). EEG and MEG coherence: measures of functional connectivity at distinct spatial scales of neocortical dynamics. *Journal of Neuroscience Methods, 166*, 41–52.

Stanfield, A.C., McIntosh, A.M., Spencer, M.D., Philip, R., Gaur, S., Lawrie, S.M. (2008). Towards a neuroanatomy of autism: a systematic review and meta-analysis of structural magnetic resonance imaging studies. *European Psychiatry, 23*, 289–99.

Vidal, C.N., Nicolson, R., DeVito, T.J., et al. (2006). Mapping corpus callosum deficits in autism: an index of aberrant cortical connectivity. *Biological Psychiatry, 60*, 218–25.

Villalobos, M.E., Mizuno, A., Dahl, B.C., Kemmotsu, N., Muller, R.A. (2005). Reduced functional connectivity between V1 and inferior frontal cortex associated with visuomotor performance in autism. *Neuroimage, 25*, 916–25.

von dem Hagen, E.A., Stoyanova, R.S., Baron-Cohen, S., Calder, A.J. (2013). Reduced functional connectivity within and between 'social' resting state networks in autism spectrum conditions. *Social Cognitive and Affective Neuroscience, 8*, 694–701.

von Stein, A., Chiang, C., Konig, P. (2000). Top-down processing mediated by interareal synchronization. *Proceedings of the National Academy of Sciences of the United States of America, 97*, 14748–53.

von Stein, A., Sarnthein, J. (2000). Different frequencies for different scales of cortical integration: from local gamma to long range alpha/theta synchronization. *International Journal of Psychophysiology, 38*, 301–13.

Wang, X.J. (2010). Neurophysiological and computational principles of cortical rhythms in cognition. *Physiological Reviews, 90*, 1195–268.

Wing, L., Leekam, S.R., Libby, S.J., Gould, J., Larcombe, M. (2002). The Diagnostic Interview for Social and Communication Disorders: background, inter-rater reliability and clinical use. *Journal of Child Psychology and Psychiatry, and Allied Disciplines, 43*, 307–25.

Wolff, J.J., Gu, H., Gerig, G., et al. (2012). Differences in white matter fiber tract development present from 6 to 24 months in infants with autism. *The American Journal of Psychiatry, 169*, 589–600.